



HAL
open science

On the nature of motor planning variables during arm pointing movement: Compositeness and speed dependence

Van Hoan Vu, Brice Isableu, Bastien Berret

► **To cite this version:**

Van Hoan Vu, Brice Isableu, Bastien Berret. On the nature of motor planning variables during arm pointing movement: Compositeness and speed dependence. *Neuroscience*, 2016, 328, pp.127-146. 10.1016/j.neuroscience.2016.04.027 . hal-04262413

HAL Id: hal-04262413

<https://hal.science/hal-04262413>

Submitted on 27 Oct 2023

HAL is a multi-disciplinary open access archive for the deposit and dissemination of scientific research documents, whether they are published or not. The documents may come from teaching and research institutions in France or abroad, or from public or private research centers.

L'archive ouverte pluridisciplinaire **HAL**, est destinée au dépôt et à la diffusion de documents scientifiques de niveau recherche, publiés ou non, émanant des établissements d'enseignement et de recherche français ou étrangers, des laboratoires publics ou privés.

ON THE NATURE OF MOTOR PLANNING VARIABLES DURING ARM POINTING MOVEMENT: COMPOSITENESS AND SPEED DEPENDENCE

VAN HOAN VU,^{*} BRICE ISABLEU AND BASTIEN BERRET

^a CIAMS, Univ. Paris-Sud., Université Paris-Saclay, 91405 Orsay, France

^b CIAMS, Université d'Orléans, 45067 Orléans, France

Abstract—The purpose of this study was to investigate the nature of the variables and rules underlying the planning of unrestrained 3D arm reaching. To identify whether the brain uses kinematic, dynamic and energetic values in an isolated manner or combines them in a flexible way, we examined the effects of speed variations upon the chosen arm trajectories during free arm movements. Within the optimal control framework, we uncovered which (possibly composite) optimality criterion underlays at best the empirical data. Fifteen participants were asked to perform free-endpoint reaching movements from a specific arm configuration at slow, normal and fast speeds. Experimental results revealed that prominent features of observed motor behaviors were significantly speed-dependent, such as the chosen reach endpoint and the final arm posture. Nevertheless, participants exhibited different arm trajectories and various degrees of speed dependence of their reaching behavior. These inter-individual differences were addressed using a numerical inverse optimal control methodology. Simulation results revealed that a weighted combination of kinematic, energetic and dynamic cost functions was required to account for all the critical features of the participants' behavior. Furthermore, no evidence for the existence of a speed-dependent tuning of these weights was found, thereby suggesting subject-specific but speed-invariant weightings of kinematic, energetic and dynamic variables during the motor planning process of free arm movements. This suggested that the inter-individual difference of arm trajectories and speed dependence was not only due to anthropometric singularities but also to critical differences in the composition of the subjective cost function. © 2016 IBRO. Published by Elsevier Ltd. All rights reserved.

Key words: arm movement, speed-dependence, optimal control, composite cost, motor planning.

*Correspondence to: V. H. VU, STAPS, Bâtiment 335, 91405 Orsay Cedex, France.

E-mail address: vuhoan.anco@gmail.com (V. H. Vu).

Abbreviations: CNS, central nervous system; DoF, degrees-of-freedom; IOC, inverse optimal control; NLP, nonlinear programming problem; OCP, Optimal control problem.

INTRODUCTION

Understanding how the brain controls 3D arm movement is a long-standing issue in motor neuroscience. The complexity of the musculoskeletal system is such that the accurate achievement of athletic tasks but also of the most basic daily life activity constitutes a challenging problem. In particular, the anisotropic distribution of mass, gravity, and interaction torques acting on all degrees of freedom make the upper-limb dynamics highly nonlinear but the brain seemingly overcomes those difficulties effortlessly. Coping with such a complexity requires efficient control strategies and, therefore, the central nervous system (CNS) might internally represent or monitor some critical variables to implicitly value skilled movements such as baseball pitching, overarm throwing or just placing a cup of coffee on a table. What is the exact nature of these variables and computational rules underlying the selection of one trajectory among the infinity of possible trajectories, and whether cells in the motor cortex encode dynamic, kinematic separately or a combination rule of such variables during movement planning remain questionable even though the issue was extensively investigated in neurophysiological studies (Georgopoulos et al., 1982; Mussa-Ivaldi, 1988; Kalaska et al., 1989). In general, tackling this problem is tricky because kinematic and kinetic quantities are tightly linked by the equations of motion and many sensorimotor transformations, through internal models (Kawato et al., 1987; Wolpert et al., 1995), may occur within the CNS before a goal-directed movement is eventually triggered. This question was nonetheless addressed in many behavioral and computational studies, but whether the control of upper-limb motion relies more upon geometrical properties pertaining to the position of body segments and joint angles (i.e. kinematic variables) or upon mechanical properties pertaining to the mass distribution and torques (i.e. dynamic variables) is still a matter of debate (Pagano and Turvey, 1995; Wolpert et al., 1995; Soechting and Flanders, 1998; Darling and Hondzinski, 1999). Isableu et al. (2009) showed that, during a cyclical upper-limb rotation task with a flexed arm ("L-shaped"), subjects exhibited spontaneous changes of rotation axis, switching from a geometrical one (Shoulder–Elbow axis, SE, a kinematic-related parameter) to an inertial one (minimum principal inertia axis, e3, a dynamic-related parameter) when executing the task at a larger speed. Hence, this suggested that the variables represented by the brain to control unrestrained 3D arm movement might combine both kinematic

and dynamic parameters and that, importantly, their interplay may depend on speed.

Interestingly, the optimal control framework precisely makes hypotheses about the variables potentially represented by the brain during motor control (Todorov, 2004). Therefore, the question of which variables are the subject of motor planning can be rephrased in a normative way as follows: what is the nature of the optimality criterion underlying trajectory formation? (see Soechting and Flanders, 1998). In this context, some researchers have argued for kinematic-oriented motor planning (in either extrinsic or intrinsic space) where the nonlinearities of the motion dynamics are just compensated for or suppressed by the brain to preserve limb's stability (Hollerbach and Flash, 1982; Atkeson and Hollerbach, 1985; Sainburg et al., 1995, 1999; Bastian et al., 1996; Gribble and Ostry, 1999). The main advantage of using a kinematic-based motor control would be to simplify control and allow the brain (re)using a common motor pattern to perform movements at various speeds (i.e. "scaling law"). This approach found some experimental support in the literature (Atkeson and Hollerbach, 1985; Gribble et al., 1998). According to this view, speed-independent arm trajectories should be observed (and were actually observed to some extent in several arm reaching studies, e.g. Atkeson and Hollerbach, 1985; Gribble et al., 1998). Other authors have instead argued for dynamic-oriented motor planning where the mechanical limb properties are taken into account and exploited to the greatest extent possible (Dounskaia et al., 2002; Debicki et al., 2010, 2011; Hore et al., 2005, 2011). The advantage would be to utilize all the non-muscular torques originating from the nonlinearities of the limb's dynamics for producing least effort movements and somehow reducing the overall amount of muscle torque (or its mechanical work) to a minimum (Sainburg and Kalakanis, 2000; Dounskaia et al., 2002; Galloway and Koshland, 2002; Hirashima et al., 2007; Berret et al., 2008; Gaveau et al., 2011, 2014). In Wolpert et al. (1995), the authors directly addressed the issue about whether the brain controls movement in kinematic or dynamic coordinates for visually guided movements. They showed that the planning of constrained planar arm reaches was associated with the optimization of a kinematic cost function (i.e. Cartesian jerk) in order to perceive straight endpoint displacements on a screen. However it is known that unrestrained or 3D movements may have very different characteristics (Desmurget et al., 1997; Gielen, 2009) and whether the control of free arm movements also relies more upon kinematic rather than upon dynamic variables remained unclear. For 3D arm movements, evidence was found for a dynamic level of planning as the final arm posture was shown to depend on the initial arm posture in a way that could not be accounted for by any kinematic optimality criterion (Soechting et al., 1995). However, the effect of speed onto the final posture selection, which is a crucial assessment to distinguish between kinematic and dynamic strategies, has not been addressed in that study but experimental studies later revealed an invariance of the final whole-arm configuration with respect to motion velocity (Nishikawa et al.,

1999) despite the fact that dynamic motor planning may potentially involve trajectory modifications with respect to speed because of the complex velocity and acceleration-dependent musculoskeletal dynamics.

To reconcile all these findings, the idea of composite cost functions relying upon kinematic, energetic and dynamic variables emerged as a possible avenue. Using inverse optimal control techniques for unveiling optimality criteria and/or rule from experimental trajectories (Mombaur et al., 2009; Berret et al., 2011b) and the free reach-endpoint paradigm for better discriminating between candidate cost functions (Berret et al., 2011a,b, 2014), it was shown that vertical movements starting from different initial positions and executed at a relatively fast pace could be accounted for by a composite cost mixing the angle jerk (i.e. a kinematic variable) and the absolute work (i.e. an energetic variable). However, it remained unclear whether these results would extend to 3D motion and whether a single composite cost could explain movements executed at different speeds. This question is also critical in regards to the understanding of self-paced movements where a cost of time may also combine with trajectory costs and the extent to which the latter varies according to speed instructions is a related open question (see Shadmehr, 2010; Shadmehr et al., 2010; Berret and Jean, 2016).

Here we combined a specific motor task with an inverse optimal control methodology to address the above questions. First, we considered free 3D arm movements without a prescribed reach endpoint (the hand could freely move in 3D), which differs from classical point-to-point reaching paradigms; namely we considered a planar target. Thus, participants were free to choose any final finger position on the target plane while only caring about the vertical error (i.e. the task goal). Considering a 4-dof arm, the subjects were thus left with three angles to choose at the movement end. A real life example of this laboratory experiment would be that of placing a cup on an empty table or pushing a door for opening it. Furthermore, we varied the instructed speed to emphasize differences between kinematic versus dynamic control strategies or combination of them and used inverse optimal control techniques to identify the elementary components of the cost function among kinematic, energetic and dynamic quantities as well as their relative weights and speed dependence.

EXPERIMENTAL PROCEDURES

Experimental task

Participants. Fifteen healthy subjects (7 women and 8 men) voluntarily agreed to participate in the experiment. Written informed consent was obtained from each participant in the study as required by the Helsinki declaration and the EA 4042 local Ethics Committee. All of them were right-handed, free of sensory, perceptual and motor disorder, aged 27 ± 4 years, weighted 66 ± 8 kg and 167 ± 6 cm tall. All the participants were naive to the purpose of the experiment.

Free endpoint motor task. The motor task is illustrated in Fig. 1. A small solid stick serving as a reference position for the initial fingertip position was attached to a vertical slider bar, allowing the experimenter to adjust appropriately the height of this reference point relative to the arm's length of each participant. A uniform horizontal surface, made of a thin and soft block of foam, served as a target throughout this experiment. It was positioned on a table just below the participant's chest. On the wall in front of the participants, a yellow marker was positioned to fix gaze in a predefined direction (looking straight ahead). Gaze was constrained in order to reduce the influence of visuomotor processing during arm movement control and to limit possible inter-trial and inter-individual fluctuations due to eye motion and eye-head-hand coordination. Participants sat comfortably on a chair with their back tighten upright against the chair's splash to freeze motion of other body parts during the execution of arm movement. The initial arm configuration was setup such that the shoulder–elbow axis was approximately abducted to the horizontal while the flexion–extension elbow angle was actively held at 90° and the fingertip was kept strictly to the reference position. Participants were free to rotate their shoulder and elbow in 3D space during the motion, but their wrist rotation was constrained by two lightweight bars attached to the distal part of the forearm and the proximal part of hand.

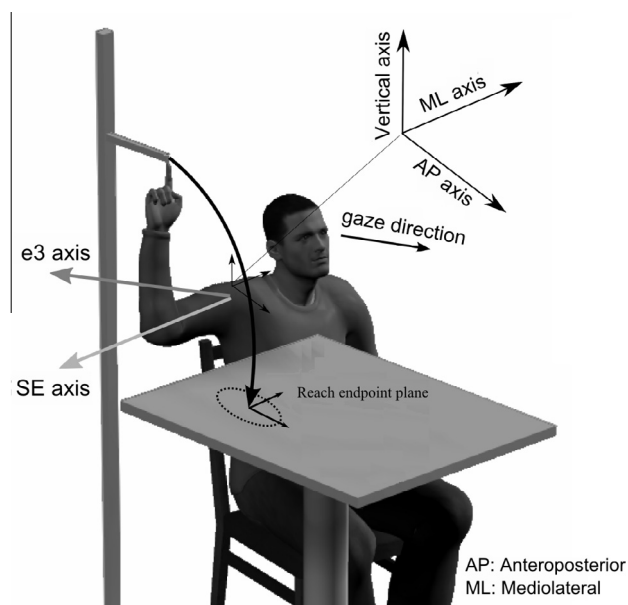


Fig. 1. Illustration of the experimental paradigm. Fixed initial arm position and horizontal target plane were tested, thereby defining a free reach-endpoint motor task. The reach endpoint was one prominent movement parameter. Two other relevant movement parameters (rotation axis displacements, SE and e3) are depicted. Gaze direction was controlled during the movement as indicated by the arrow. Note that any possible path leading to any location onto the surface was possible regarding task achievement. The task was thus redundant (3 free joint angles for most endpoint locations) and 3D as the arm could freely move in 3D space without any constraint, except that of reaching the target plane at various instructed speeds (slow, normal and fast, denoted by S, N and F respectively).

One of the two bars also froze the movement of the index finger. Such constraints allowed to approximate the forearm and the hand as a single rigid body and to simplify the whole-arm model by reducing the actual arm's degrees-of-freedom (DoF) from seven to five (three at shoulder and two at elbow). In practice, only the first four DoFs were relevant because the elbow pronation/supination rotation showed negligible displacements in this study and was irrelevant to the pointing task under consideration (fingertip end-effector). We therefore considered a 4-DoF arm model in this study. Note that with a 4-DoF arm and a planar target, the task is redundant: for a given admissible fingertip position of the target plane (which is chosen by the subject himself), three joint angles can be freely adjusted. If we had use a dot as a target, only one angle could have been selected for the prescribed reach endpoint. Hence the main originality of the present protocol is to let subjects solve the “where to go” problem as well as the “how to go there” problem at once, which is a common situation (e.g. putting a cup of coffee on an empty table is an analog of such a laboratory experiment).

During the experiment, participants were instructed to move their fingertip from the initial configuration to the destination (i.e. a uniform planar target, with no prescribed reach endpoint) by performing a smooth, one-shot movement while looking at the eyes reference marker. They were required to point to the planar surface with their fingertip and stop their motion right onto the surface but without hitting it. No instruction was given to the participants regarding the final position of the fingertip on the planar surface. As such, all reach endpoints were equi-efficient regarding task achievement but conceivably not equi-efficient regarding the subjective values associated with the actual arm trajectory leading to the chosen reach endpoint (see also Berret et al., 2011a,b, 2014 for related studies). Here and throughout the paper, subjective costs (i.e. costs not imposed by the task but related to the subject or body) will be contrasted with objective costs that are imposed by the task itself (e.g. pointing error) (Berret et al., 2011b; Knill et al., 2011).

For the purpose of this study, three different speeds were examined: slow (S), comfortable/natural (N) and fast (F). Before each trial, participants were verbally instructed to move at one specific speed. Speed instruction was randomized across trials in order to prevent habituation and memorization effects (especially regarding the endpoint reached in the previous trial). Velocity constraints were hypothesized to reveal the nature of the planning variables used in such 3D movements, and the free reach-endpoint paradigm was used to emphasize the possible differences of arm trajectories as a function of the instructed speed.

Prior to the experiment, participants were trained to become familiar with the task. They were told to move their arm toward the target while the experimenter verified that all the task instructions had been well understood. The training process consisted of 20 trials on average and at the end all the participants had the

capability of executing their movement while satisfying the experimental instructions, which were as follows: (i) place consistently the fingertip at the initial reference position while keeping the same initial “L-shaped” arm posture, (ii) try to stop the movement right onto the horizontal target surface, by minimizing errors along the vertical axis, (iii) look at the reference marker during the whole movement execution and (iv) mark a clear difference of motion speed based upon the verbal instruction given by the experimenter at the beginning of trial.

For each participant, 15 trials were recorded per speed. Thus, a total number of 675 trials (15 trials \times 3 speeds \times 15 participants) were recorded and used for subsequent analyses in the study. During the experiment, participants were allowed to rest in order to minimize fatigue effects. The duration of the experiment was approximately 45 min per participant.

Data collection and processing

Materials. An optical motion capture system consisting of eight high-speed cameras was used to record the arm motion at a frequency of 250Hz (Vicon motion system Inc. Oxford, UK). A set of plug-in-gait markers was attached to the participant body. Precisely, thirteen markers were placed at well-defined anatomical locations on the dominant arm and the other parts of the body, namely: seventh cervical vertebrae, 10th thoracic vertebrae, clavicle, sternum, right and left acromion, lateral and medial humeral epicondyles, ulnar and radial styloids, 2nd and 5th metacarpal heads and 1st fingertip.

Motion analysis. All the analyses were performed with custom software written in Matlab (Mathworks, Natick, MA, USA) from the recorded three-dimensional position of the markers. The recorded positional data were first smoothed using a 2nd-order Butterworth low-pass filter with cut-off frequency at 10Hz and then processed to compute other kinematic and dynamic parameters, as described hereafter.

Kinematic-level analysis. Hand kinematics. For every recorded trial, the position of the fingertip marker was numerically differentiated to obtain the corresponding velocity profile. Based on this velocity profile, the movement duration (MD) was estimated by the time window where the velocity magnitude was above 5% of the peak velocity. Other kinematic parameters relevant to the purpose of the present study were then computed and analyzed to check for differences in hand kinematics with respect to the instructed speed, as follows: the reach endpoint location in 3D (RE, described by its Cartesian coordinates X, Y and Z with respect to a frame whose origin is located at the shoulder joint), the peak velocity (PV), accuracy and precision along the vertical axis (denoted by Za and Zp, respectively). In practice, Za was defined based on the distance from the final finger position to the planar target and Zp was defined as the standard deviation of the vertical RE coordinates. They were used to verify constant and variable errors along the vertical axis. Note that, in the present task, Xa and Ya were undefined as

the task did not impose any final fingertip position in the plane. Finally, Xp and Yp were analyzed via 95% confidence ellipses showing the distributions of RE within the target plane.

Joint kinematics. The 4-DoF arm configuration was computed from the recorded motion data. To this aim, we employed the method previously described in [Isableu et al. \(2009\)](#). Briefly, this method considered the 3D arm as an articulated chain of rigid bodies connected by joints. Then, a local segment coordinate system was calculated based on the measured 3D position of the markers in a way that was consistent with the International Society of Biomechanics (ISB) recommendation ([Wu et al., 2005](#)). From the resulting coordinates, rotation matrices converting a specific coordinate to its parent coordinate were computed in accordance with the rotation orders, which allowed angles to remain as close as possible to the clinical definition of joint and segment motion. Based on these calculated rotation matrices, the values of (Euler) rotation angles (internal/external, elevation/depression, ulnar/radial at shoulder and extension/flexion at elbow) were easily inferred. Again, the joint velocities and accelerations were obtained by numerically time-series differentiating the angular displacements.

Dynamic-level analysis. Inverse dynamic analysis was used to estimate the muscle torques underlying the observed motion kinematics. A dynamical model of the arm was required to infer these movement parameters. As mentioned above, the arm was viewed as the combination of rigid bodies connected by series of revolute joints. If such a model can be easily established for planar systems (e.g. [Berret et al., 2011b](#)), the task is more tedious in 3D especially when computational efficiency really matters. Thus, special considerations were taken into account. Firstly, the series of arm rotation axes as well as the segment coordinates in Wu's model ([Wu et al., 2005](#)) were re-approached within the standard robotic point of view wherein the four rotation axes were re-described using Denavit–Hartenberg parameters. The same description could be found for instance in [Asfour and Dillmann \(2003\)](#), where the robotic model of a humanoid arm was described. From this formalism, many of the advanced tools developed in robotics could be applied to calculate both forward or inverse kinematic and dynamic parameters. Secondly, another crucial piece was the anthropometric parameters. The parameters reported in [Dumas et al. \(2007\)](#) were used, providing us with an approximation of anthropometric values such as mass, center of mass position and inertia matrix for each segment. These parameters were adjusted for each participant given his/her total mass and the lengths of the body segments (measured via motion capture).

From a classical application of Lagrange mechanics, the arm skeleton dynamics can be expressed as follows:

$$\tau = \mathcal{M}(\theta)\ddot{\theta} + \mathcal{C}(\theta, \dot{\theta}) + \mathcal{G}(\theta) + \mathcal{R}(\theta, \dot{\theta}), \quad (1)$$

where τ is the muscle torque, \mathcal{M} is the mass matrix (4×4 size here), \mathcal{C} is the Coriolis and centripetal torque, \mathcal{G} is the gravitational torque. Note that computed in this way, the muscle torque is actually affected by some term $\mathcal{R}(\theta, \dot{\theta})$ reflecting frictional and viscous or elastic torques created

by all soft tissues. In the current work, the latter term \mathcal{R} was neglected and assumed to be negligible compared to the other torques. The vector $\theta = (\theta_1, \dots, \theta_4)$ denotes the four angles describing the arm's configuration and a dot above a variable stands for its time derivative.

We may subsequently define the muscle, net, interaction and gravitational torques as follows:

$$\begin{aligned}\tau_{mus} &= \tau, \\ \tau_{net} &= \text{diag}(\mathcal{M}(\theta))\ddot{\theta}, \\ \tau_{int} &= -[(\mathcal{M}(\theta) - \text{diag}(\mathcal{M}(\theta)))\ddot{\theta} + C(\theta, \dot{\theta})], \\ \tau_{gra} &= -\mathcal{G}(\theta).\end{aligned}$$

where $\text{diag}(\mathcal{M}(\theta))$ represents the diagonal matrix built from the diagonal terms of the mass matrix. Then, Eq. (1) can be rewritten as follows:

$$\tau_{net} = \tau_{mus} + \tau_{int} + \tau_{gra}, \quad (2)$$

which is similar to the description given in Yamasaki et al. (2008) and Sande de Souza et al. (2009). In particular, this shows that the net torque at each joint is produced by a combination of muscle torque, interaction torque and gravitational torque.

In practice, the above analytic formulas are quite long to evaluate explicitly and using them is therefore computationally inefficient for intensive simulations. Hence we used a recursive Newton-Euler algorithm to compute the arm dynamics in our simulations. State-of-the-art algorithms for rigid body dynamics can be found in Featherstone and Orin (2000). Actually, by replacing 3D vectors by 6D spatial vectors in the classical Newton-Euler recursive algorithm, efficiency of the arm's dynamics calculation could be largely improved (for both direct and inverse dynamics). Computational efficiency was especially crucial in the present study because optimal control methods involve very intensive computations and numerous evaluations of the arm's dynamics (see below). We actually checked that both methods to calculate the dynamics (either based on Lagrangian or Newton-Euler formalisms) gave the same result but the latter was about 10 times faster than the former in our settings (note that a compiled version of the code provided by Featherstone and Orin (2000) was eventually used for better efficiency).

Global motion parameters. In this study, three indexes summarizing different aspects of the overall arm motion were analyzed. Most of them were discussed in previous papers (Pagano and Turvey, 1995; Riley and Turvey, 2001; Sainburg and Kalakanis, 2000; Isableu et al., 2009), which is the reason why our analysis will rely upon them. The first parameter is the reach endpoint index (RE index); the second and third indexes respectively the average deviation of the shoulder–elbow axis (SE index, i.e. kinematic parameters) and the average deviation of the minimum inertia axis (e3 index, i.e. a kinetic parameter).

Antero-posterior reach endpoint position (RE index). The RE index was defined as the final fingertip position on the planar target along the AP axis (X_{AP}) normalized by the maximal distance that the participant could reach to without moving/bending the trunk (D_{max} ,

corresponding to a fully extended arm such that the fingertip was on the target plane).

$$\text{RE index} = \frac{X_{AP}}{D_{max}} \times 100. \quad (3)$$

Minimum principal inertia axis deviation (e3 index).

This dynamic parameter is based on the minimum principal inertia axis (referred to as e3 in previous studies). A method to calculate the instantaneous e3 axis during a 4-DoF arm movement was described in Isableu et al. (2009). Importantly, it is worth noting that e3 definition only relies on the instantaneous whole-arm configuration and its anthropometric characteristics. At each time step, the angle between the current e3 axis direction and its initial ($t = 0$) one, $a_{e3}(t)$, was computed and the e3 index was calculated as in Eq. (4).

$$\text{e3 index} = \frac{1}{T} \int_0^T |a_{e3}(t)| dt. \quad (4)$$

A strict rotation around e3 axis would thus indicate a strategy exploiting the inertial properties of the arm (when viewed as a single “L-shaped” rigid body). Indeed, the task could be performed by strictly rotating the arm around e3 axis, with no forearm flexion/extension. Intuitively, such a strategy could facilitate the production of large angular accelerations at equivalent muscle torque magnitude. For instance, rotating the arm around the maximum principal inertia axis would lead to smaller acceleration for similar muscle torque, which is just the result of the intrinsic inertial properties of an arm in such a L-shape configuration. Moreover, rotating around e3 may be advantageous because the angular momentum then becomes parallel to the angular velocity vector of the rigid body and therefore a muscle torque around e3 only produces angular acceleration around e3 without inducing accelerations around other axis (i.e. interaction torques).

Shoulder–elbow deviation index (SE index). The SE index was defined as the mean integral of the absolute shoulder–elbow axis deviation. At each time step, the angle between the current shoulder–elbow axis direction and its initial (at $t = 0$) one, $a_{SE}(t)$, was computed and the SE index was calculated as reported in Eq. (5):

$$\text{SE index} = \frac{1}{T} \int_0^T |a_{SE}(t)| dt \quad (5)$$

where T was the total movement duration (obtained experimentally for each trial). A strict rotation around this axis when performing the task was possible, yielding a SE index equal to zero. In turn, this would indicate the use of a kinematic control strategy possibly aiming at stabilizing the upper arm segment during the whole motion (Isableu et al., 2009).

Optimal control modeling and inverse optimal control method

In this section, we describe the optimal control methods and the numerical inverse optimal control approach that we used. The method follows the works of Mombaur et al. (2009) and Berret et al. (2011b), and aims at accounting for the 3D arm motion from an optimal control

standpoint by finding the subjective costs underlying the experimental trajectories. The control dynamics, denoted by noted (Σ), is formed of the skeletal dynamics given in Eq. (1) and some basic muscle dynamics. Muscle dynamics was added here to account for the smoothness of velocity and acceleration signals and was not assumed to be an accurate model of the muscle–tendon complex. Therefore, we used a simple model accounting for the low-pass filter property of muscles, as it is quite common in optimal control studies (e.g. Uno et al., 1989; Guigon et al., 2007; Berret et al., 2011a). Precisely, we assumed that the motor command (i.e. control signal) was simply the derivative of the muscle torque, as follows:

$$\dot{\tau} = \mu \quad (6)$$

where the control μ can be thought as the overall motor input given to the muscle.

Solving an optimal control problem with non-linear dynamics and non-quadratic cost functions is generally a difficult problem especially for problems with large dimensions (here the state vector had 12 dimensions and the control vector had 4 dimensions). One could however observe that the limb and muscle dynamics together form a fully-actuated control system that is feedback linearizable. Therefore, it was possible to effectively change the nonlinear control problem into a linear control problem by directly controlling the derivative of the angular acceleration vector instead of the derivative of the muscle torque. This mathematical change of control variable allowed us to replace Eq. (6) with the following one:

$$\ddot{\theta} = \mu \quad (7)$$

The muscle torque (and its derivative) could then be recovered via inverse dynamics (see above). Even though we could control μ directly, we generally observed that such approach yielded faster and more robust convergence during the numerical resolution of the optimal control problems under consideration. The numerical difficulties were then left to the possible non-quadraticity of the cost function.

In the literature, several cost functions were proposed by different authors. It is useful to distinguish subjective and objective cost functions. Subjective costs differ from objective ones in that the former reflect a subject's decision/choice while the latter are imposed by the task (e.g. accuracy). Here we focus on the identification of subjective costs only. Various subjective cost functions were proven useful and relevant as it often replicated at least some experimental observations. Briefly, previously proposed cost functions may be grouped into three main categories: kinematic, energetic and dynamic. All classes with one relevant representative cost are listed in Table 1. Here we considered the minimum angle jerk (Wada et al., 2001) to represent the kinematic cost family (we could have used a minimum acceleration criterion (Ben-Itzhak and Karniel, 2008) but the predictions of the two models only differed slightly). For the dynamic class, we considered the minimum torque change model (Uno et al., 1989). We also tested the minimum torque model (Nelson, 1983) but we found

Table 1. Cost functions considered in this article. Their overall class (kinematic, energetic or dynamic), the chosen representative element of each class with its classical name, the mathematical definition of the cost and the references which proposed them

Class	Criterion	Cost function	References
Kinematic	Angle jerk	$C_{Kine} = \int_0^T \sum_{i=1}^4 \ddot{\theta}_i^2 dt$	Wada et al. (2001)
Energetic	Absolute work	$C_{Ener} = \int_0^T \sum_{i=1}^4 \dot{\theta}_i \tau_i dt$	Nishii and Murakami (2002) and Berret et al. (2008)
Dynamic	Torque change	$C_{Dyna} = \int_0^T \sum_{i=1}^4 \dot{\tau}_i^2 dt$	Uno et al. (1989) and Nakano et al. (1999)

that the torque change model was more relevant for the present motor task. At last, at the interface between kinematic and dynamic variables are energetic costs that measure actual energy expenditures associated with the movements. We chose the minimum absolute work of muscle torques here (Berret et al., 2008; Gauthier et al., 2010; Gaveau et al., 2014). The geodesic (Biess et al., 2007) or the minimum peak work model (Soechting et al., 1995) are other models that could have been considered within this class but their exact formulation is less easily integrable within a generic optimal control scheme, which may be problematic for running inverse optimal control (see below).

Although each of the above cost function was proved to be effective under specific conditions, it is actually very difficult and likely impossible to identify a unique and generic cost function that will account well for all possible human arm movements. It may thus seem reasonable to widen the optimal control hypothesis and investigate the idea of composite cost functions. In this vein, recent work (Berret et al., 2011b) showed that free arm pointing movement could not be explained by any single cost among a variety of 7 possible candidates but by the combination of mainly two of them, namely angle jerk and absolute work optimality criteria. Based on these prior findings and because of the computational load and complexity of the present 4-DoF arm model we restricted our analysis to the combination of the three cost functions listed in Table 1, which we shortly refer to as kinematic (Kine), energetic (Ener) and dynamic (Dyna) throughout the study. Thus, the composite cost function may be written as:

$$C(\alpha) = C_{Kine} + \alpha_1 C_{Ener} + \alpha_2 C_{Dyna} \quad (8)$$

The triplet $\alpha = (1, \alpha_1, \alpha_2)$ uniquely determines the composite cost function. We will refer to α as the weighting vector (whose elements are non-negative). The factor 1 in the first component of the triplet is due to the fact that the composite cost can be normalized (see Mombaur et al., 2009; Berret et al., 2011b). Our investigations showed that the kinematic cost was relevant and necessarily present to account for the subject's behavior. Considering 3 costs (and thus having only 2 free parameters) also enabled convenient visualization possibilities (see Results).

It is noteworthy that for each participant three different speeds (S, N, F) were studied in the current work. In order to find the composite cost functions that best replicated the recorded data, two solutions were available. Firstly, one could try to find a composite cost corresponding for each speed, thereby assuming that task instructions could affect the weights of the subjective cost. We thus termed this type of cost “speed-dependent composite costs” and denoted it by SDComp. Alternatively, one could also try to find a single composite cost accounting for all speeds at once. We termed this type of cost “speed-independent composite cost” and denoted it by SIComp. These two possible hypotheses make divergent assumptions regarding the flexibility of subjective costs with respect to task instructions. The results of both SDComp and SIComp costs will be compared to determine which one is the more plausible following Occam’s razor principle (for similar accuracy, the most parsimonious model should be retained).

Optimal control problem (OCP). The OCP corresponding to the cost $C(\alpha)$ can be stated as follows: Find an optimal control \mathbf{u}_α^* and its corresponding optimal trajectory $\mathbf{q}_\alpha^{\star T} = (\theta^T, \dot{\theta}^T, \ddot{\theta}^T)$ of system (Σ) , connecting a source point \mathbf{q}_s to a final point on the target plane in time T and yielding a minimal value of the cost $C(\alpha)$ (then denoted by $C^*(\alpha)$).

To solve this problem, the Matlab software GPOPS (Rao et al., 2010) was used. This method employs an orthogonal collocation technique to convert the continuous time OCP into a nonlinear programming problem (NLP) with constraints. The well-established numerical software SNOPT was used to solve the NLP problem. For each simulation, the angular velocity and acceleration at initial and final times were set to zero since the participants were required to start and stop their motion with a static state. The other parameters such as the initial angular configuration θ_0 and the motion duration T were directly estimated from the recorded data. The anthropometric parameters such as inertia, mass, center of mass, segment length were customized for each participant, thereby accounting for physical inter-individual differences.

Inverse optimal control (IOC). Inverse optimal control problem was stated as a bi-level problem with an outer loop seeking for the α best fitting the recorded trajectories, and an inner loop that finds the optimal trajectory for the current α (see also Mombaur et al., 2009; Berret et al., 2011b for details).

Importantly, a function (or metric, denoted by Φ) to compare simulated and recorded arm trajectories is needed. Here, we sought for a vector α allowing to replicate at best the recorded four angles in the joint space. At the initial time, the simulated and recorded angles (respectively denoted by \mathbf{q}_α^* and \mathbf{q}^{meas}) coincided perfectly, but differences typically appeared during the course of motion. The function used to measure this discrepancy was defined as the maximal deviation of the simulated angular displacements from the reference ones (simply taken as the average experimental values observed for each speed condition). Note that this metric was quite conservative as it involved the maximal

deviation and not the averaged one. Eventually, four deviations corresponding to the four joint angles were obtained, which were averaged to get a single overall error in joint space, denoted by $E_{Joint}(\alpha)$. Different values of E_{Joint} were obtained for different values of α_1 and α_2 , hence this error could be visualized using 3D plots (see Results).

Therefore, by definition, $\Phi(\mathbf{q}_\alpha^*, \mathbf{q}^{meas}) = E_{Joint}(\alpha)$ for the SDComp case. For the SIComp case, the metric was modified to minimize the error for all 3 speeds together (the average was simply used). The purpose of the outer loop is to minimize this error (Φ) by finding the best α , that is, the best-fitting cost combination for replicating the experimental data (for each speed separately for SDComp and for all speeds simultaneously for SIComp).

To solve this part of the problem, a method called CONDOR standing for Constrained, Non linear, Direct, parallel optimization was used. A re-scaling method described in Berret et al. (2011b) was also needed in the present work to improve the efficiency of the algorithm (due to the different units and order of magnitudes of the costs). In addition, the value of α or $\bar{\alpha}$ was initialized with random non-negative values and 10 random restarts were considered for each inverse optimal control problem and for each participant in order to limit the issue of being stuck at a local minimum. The best α were eventually chosen as the ones that made the function Φ as small as possible. In total applying this procedure to all the participants required solving 450 IOC problems (10 restarts \times 3 speeds \times 15 participants) for the SDComp case and 150 IOC problems (10 restarts \times 15 participants) for the SIComp case.

Cost contribution calculation. We used the formula originally described by Berret et al. (2011b) to evaluate the contribution of each cost function to the total cost. Investigating cost contributions was interesting because the components of the vector α could not be straightforward to interpret: the largest α_i could potentially be of minor importance with respect to trajectory fitting depending on the units or order of magnitudes of each elementary cost.

Comparison between simulated and experimental trajectories. Simulated and experimental trajectories were compared in two ways: first, absolute errors were computed and, second, relative errors linked to speed variations were estimated to assess how each cost could predict the speed dependence of motor strategies.

Cartesian error of the finger trajectory. In order to estimate the accuracy of trajectory reconstructions also in Cartesian space, we computed the maximal deviation between experimental and simulated 3D finger trajectories and this Cartesian error was denoted by E_{Cart} .

Reach endpoint index error (E_{RE}). The reach endpoint error measured the distance between the recorded RE index (RE_{exp}) (simply taken as the average experimental values observed for each speed condition) and the simulated one (RE_{sim}) generated by either SDComp or SIComp or each of the three elementary costs. The E_{RE} values were computed for each speed and each subject.

e3 index error (E_{e3}). Similarly to the E_{RE} , the $e3$ index error measured the distance between the recorded $e3$ index ($e3_{exp}$) and the simulated one ($e3_{sim}$).

RE or e3 slope errors ($E_{\bar{K}_{RE}}$ or $E_{\bar{K}_{e3}}$). In order to evaluate whether simulated results were able to replicate hypothetical speed-dependences of RE and $e3$ for each subject, we also compared the experimental and simulated slopes resulting from a linear regression of each parameter with respect to the instructed speed. To normalize slope values across subjects, we did not use the value of K resulting from a regression against the real speeds of subjects because it could differ substantially across them. Instead, we used the value \bar{K} obtained when regressing against the instructed speed, i.e. S, N, and F labels. We then defined the speed-dependence error as the absolute difference between \bar{K}_{exp} and \bar{K}_{sim} . The analysis was done for both RE and $e3$ parameters, thus leading to the definition of $E_{\bar{K}_{RE}}$ and $E_{\bar{K}_{e3}}$ for parameters RE and $e3$ respectively.

Statistical analyses

Repeated-measures one-way ANOVAs were performed to assess the effect of speed on relevant movement parameters. The ANOVA's sphericity assumption (using Mauchly test) was checked, and p-values and degrees of freedom were corrected using estimates of sphericity (Greenhouse–Geisser/Huynh–Feldt). Post-hoc tests were conducted with Bonferroni corrections when appropriate (the chosen threshold was 0.05 and analyses were conducted using SPSS). We used quantile-quantile plots to visually check whether the data were normally distributed (qqplot Matlab function). Shapiro–Wilk's test was used to quantify these observations for the relevant parameters.

RESULTS

Experimental observations

Inter-individual analysis. Peak velocity and Movement duration. Repeated-measures ANOVAs were used to statistically check that subjects yielded significant differences with respect to the instructed speed. Recorded peak velocities were significantly different across S, N and F speed conditions ($F(2,28) = 74.8$, $p < 0.001$). This confirmed that the verbal instruction of speed was effective. Post-hoc analyses showed that all speeds were significantly distinct. Quantitative values are given in Table 2. The mean and standard deviation across subjects for the S, N, and F conditions were 1.0 ± 0.3 m/s, 2.1 ± 0.4 m/s and 3.4 ± 0.7 m/s respectively. A similar statistical analysis performed on movement duration showed similar results ($F(2,28) = 21.1$, $p < 0.001$).

Reach accuracy and precision. Although the task did not impose any particular point to reach to, the subjects had to control the constant error along the vertical axis. One objective of the task was thus to position the fingertip onto the target surface. Constant errors along the vertical (Z_a) were relatively small and independent of the speed, indicating that the final position constraint

Table 2. Experimental movement parameters (mean \pm std across subjects)

	S	N	F
MD (s)	0.90 \pm 0.20	0.54 \pm 0.12	0.30 \pm 0.06
PV (m/s)	1.0 \pm 0.3	2.1 \pm 0.4	3.4 \pm 0.7
$Sh_{internal/external}$ ($^{\circ}$)	10.4 \pm 7.9	11.9 \pm 8.8	12.6 \pm 8.5
$Sh_{elevation/depression}$ ($^{\circ}$)	10.1 \pm 6.4	10.4 \pm 6.0	10.4 \pm 6.2
$Sh_{ulnar/radial}$ ($^{\circ}$)	92.6 \pm 15.8	94.8 \pm 15.8	96.2 \pm 15.2
$El_{extension/flexion}$ ($^{\circ}$)	27.2 \pm 8.3	25.7 \pm 9.1	24.1 \pm 9.0
RE index (%)	83.1 \pm 9.1	81.2 \pm 9.6	79.8 \pm 8.7
$e3$ index ($^{\circ}$)	19.3 \pm 5.1	18.2 \pm 5.2	17.6 \pm 5.8
SE index ($^{\circ}$)	7.6 \pm 3.9	8.1 \pm 3.5	8.3 \pm 3.3
Z_a (cm)	0.6 \pm 0.4	0.7 \pm 0.4	0.6 \pm 0.5
Z_p (cm)	0.4 \pm 0.3	0.3 \pm 0.2	0.4 \pm 0.3

was fulfilled by all the participants. Regarding the variable error along the Z_p axis, they were of comparable magnitude with no speed effect. For X_p and Y_p , giving the distributions of reach endpoint in the target plane, analyses via confidence ellipses were conducted (see below for the RE index).

Angular excursions. The four angle excursions (shoulder's internal/external, elevation/depression, ulnar/radial, elbow's extension/flexion), averaged across subjects, are given in Table 2. The magnitude of angular displacements tended to depend on the instructed speed. Precisely, when speed increased, the shoulder angles (internal/external angle, elevation/depression angle, ulnar/radial angle) tended to increase while the elbow's extension/flexion angle tended to decrease. Repeated-measures ANOVAs did not show any significant effect of speed for the two first shoulder angles ($F(2,28) = 2.3$, $p = 0.139$; $F(2,28) = 0.08$, $p = 0.92$) but a significant effect was observed for the third shoulder and the elbow angles ($F(2,28) = 4.5$, $p < 0.05$; $F(2,28) = 16.3$, $p < 0.001$, respectively). Regarding the magnitude of angular excursions, it is interesting to note that although subjects could accomplish the task by simply rotating their arm only about the shoulder ulnar/radial axis, all subjects actually chose more complex joint displacements. Actually, while the movement was mainly achieved by rotating around the shoulder ulnar/radial axis (considered as a major axis), we also measured quite large displacements of elbow extension/flexion (about 1/3 of shoulder ulnar/radial excursion), and non-negligible amounts of shoulder internal/external, elevation/depression angular rotations. Therefore, the movement chosen by the subjects generally involved the coordinated displacement of several joints in different proportions.

SE, $e3$ and RE indexes. The above observations were further analyzed in terms of the global movement parameters described in the Materials and Methods. The mean \pm std values of SE/ $e3$ /RE indexes across all the subject were reported in Table 2. In agreement with the joint excursions, the SE index was relatively small for all speed conditions ($7.6 \pm 3.9^{\circ}$ for S; $8.1 \pm 3.5^{\circ}$ for N; $8.3 \pm 3.3^{\circ}$ for F), although it tended to slightly increase with respect to speed. Repeated-measures

ANOVAs did not reveal any significant differences for this global movement parameter index ($p = 0.23$). In contrast, both e3 and RE indexes tended to decrease with respect to speed and obtained the values of $19.3 \pm 5.1^\circ$, $18.2 \pm 5.2^\circ$, $17.6 \pm 5.8^\circ$ and $83.1 \pm 9.1\%$, $81.2 \pm 9.6\%$, $79.8 \pm 8.7\%$ for S, N, F respectively. For those parameters, repeated-measures ANOVAs revealed significant changes with respect to speed ($F(1.4,20.1) = 7.4$, $p < 0.01$; $F(2,28) = 14.8$, $p < 0.001$ for e3 and RE indexes respectively). A finer examination of RE and e3 indexes showed that some subjects exhibited more speed dependencies than others, which is analyzed below.

Intra-individual analysis. Reach endpoints. The distribution of reach endpoints projected onto the transverse plane is illustrated in Fig. 2. The data of two representative subjects were reported (S5 and S14 represent speed-sensitive subjects and speed-insensitive subjects, respectively). A qualitative inspection revealed an effect of speed for S5 but not in

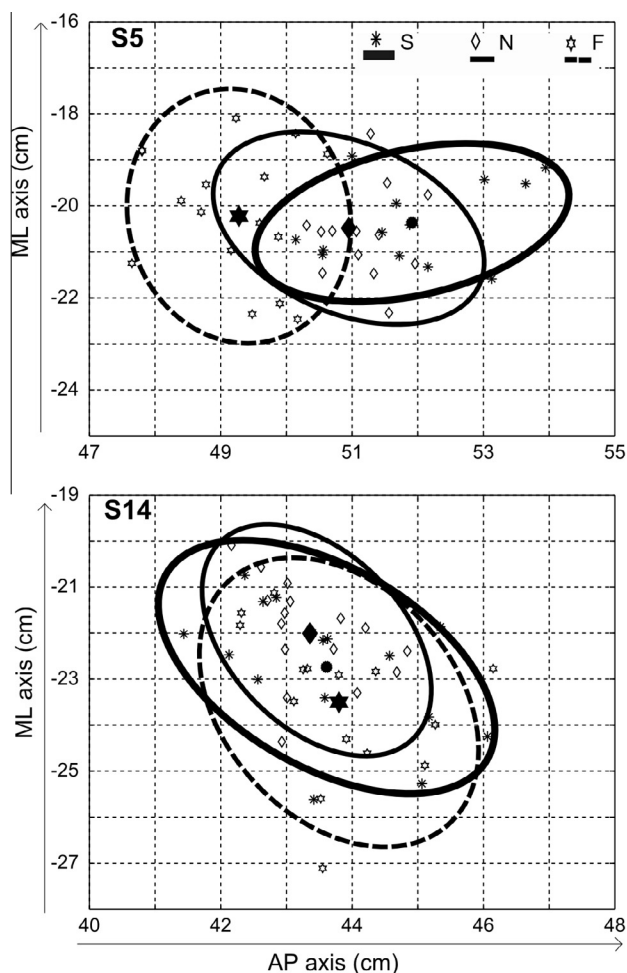


Fig. 2. Reach endpoint positions of two subjects (S5 and S14) for the three different speeds (S, N and F). The 95% confidence ellipses of reach endpoints in the S, N and F speed conditions are drawn in thick, thin and dotted lines, respectively. Note that along the antero-posterior (AP) axis, the distributions of finger positions of S14 remain relatively constant regardless of movement speed while those of S5 tend to decrease when movement speed increases.

S14. Precisely, for S5, increase of speed was accompanied by reach endpoints that tended to get closer to the shoulder location in the AP direction. Correlation analyses performed for the RE index confirmed these observations (Fig. 3). Indeed, while the RE index for S5 showed a significant negative correlation with respect to speed ($R = -0.76$, $p < 0.001$), the correlation for S14 was not significant ($p = 0.48$). The data of individual subjects are reported in Table 3 (R values, p values and K slopes are given).

e3 and SE indexes. The variations of e3 with respect to the movement speed for the two typical subjects (S5 and S14) are shown in Fig. 3 (bottom panel). Similarly to RE indexes, it is visible that the e3 index was independent of speed for S14 ($p = 0.50$) while it clearly decreased with speed increments for S5 ($R = -0.85$, $p < 0.001$). Regarding SE index (not depicted), it was increasing according to speed for S5 while speed invariant for S14 (values). The data of individual subjects are again reported in Table 3 (R values, p values and K slopes are given).

In summary, the above investigations revealed idiosyncratic behavioral strategies, with some participants using speed-dependent reach endpoints and joint trajectories while others conserved the same arm trajectories irrespective of speed instructions. Note that the use of a pointing task with unconstrained reach endpoints was essential to uncover the existence of speed-dependent strategies in some subjects. Next, to account for these experimental observations, an inverse optimal control approach is presented, which aimed at identifying the costs underlying the arm trajectories of each individual for every speed. This will prove to be useful to explain the inter-individual divergences within a unique normative framework.

Optimal control results

Reach endpoint location and rotation axis displacement as predicted by kinematic, energetic and dynamic elementary cost functions. In order to provide preliminary insights about the predictions of each elementary cost function for the present pointing task, optimal control simulation results for a subject (here S5) are shown in Fig. 4. The dependence of each single cost with respect to the required speed is also emphasized. The left panel depicts the finger's simulated movement paths while the right panel displays the variation of two global parameters (RE and e3) with respect to three speeds (S, N, F). It is noteworthy that the initialized parameters (such as the initial configuration of arm, movement durations, position of planar target) were imported directly from recorded data and kept fixed during the simulation processes. Importantly, the simulated results showed that each cost function produced different movement paths to the planar target, leading to different RE locations. For a specific movement speed (e.g. N), the kinematic cost would generate the farthest movement (i.e. more distant RE location with respect to the vertical projection of shoulder position on the planar target). Between the energetic/dynamic costs, the dynamic cost tended to

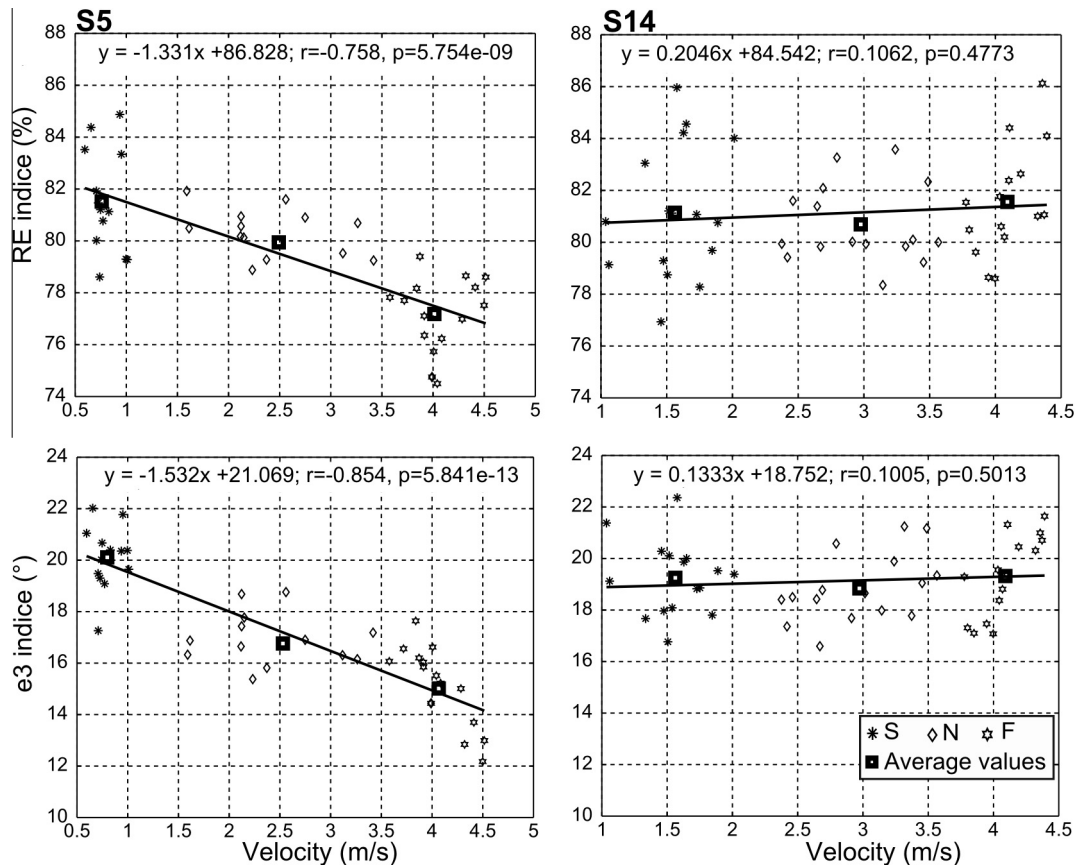


Fig. 3. Dependence of RE and e3 indexes on movement speed for the two subjects S5 (left) and S14 (right). For each examined index, linear correlation and regression lines (thin black lines) were computed based on all recorded data (each dot of the graphs corresponds to a single trial). For S14, RE and e3 indexes appear to be nearly independent of speed variations while those of S5 decrease clearly when movement speed increases.

produce the less distant RE index. Furthermore, in terms of speed dependencies, the three costs made distinct predictions: the kinematic cost did not depend on speed at all, in agreement with its theoretical foundation. However, energetic and dynamic costs exhibited some dependence on speed in both hand path curvatures and RE location. Visually, when the speed increased from S to F, the energetic cost generated quite distinguishable movement paths (smallest RE location at F speed) while the dynamic cost generated slightly different movements between speeds (but the curvature noticeably decreased with respect to speed increments). A quantitative analysis showed that the kinematic cost always produced constant RE/e3 indexes across movement speed while the energetic/dynamic costs reduced RE or e3 indexes at high or low rates when movements sped up. A finer examination of arm posture showed that the movements generated by kinematic cost mainly involved rotation about the shoulder ulnar/radial axis and negligible displacements about the other axes regardless of speed, accounting for the low values of SE index for this cost. On the contrary, the energetic/dynamic costs generated the movements that associated with all the rotational axes, yielding quite large displacements around the shoulder internal/external, elevation/depression, elbow extension/flexion

axes. Thus, one could conclude that the optimization of movement based on the sole kinematic cost could only account for speed-insensitive strategies while the optimization of pure energetic/dynamic costs should produce speed-dependent arm trajectories.

Composite cost identification. Overall fitting errors.

Composite costs were fitted to the data of each subject in order to uncover the optimality criteria underlying their experimental behaviors. In order to evaluate the performance of composite costs, their performance was systematically compared to what would be obtained using the three elementary costs separately (Kine, Ener and Dyna). For composite costs, two competing hypotheses were tested: speed-dependent vs. speed-independent composite costs (SDComp vs. SIComp, respectively). The joint space and Cartesian space fitting errors (E_{Joint}/E_{Cart} , mean \pm std values across subjects) are reported in Fig. 5. As expected, errors obtained from the best-fitting composite costs were constantly smaller than for each of the elementary costs. In joint space, the maximal angular deviations between simulated and experimental displacements were $5.5 \pm 3.2^\circ$ and $6.6 \pm 2.9^\circ$ for SDComp and SIComp, respectively. Those values were nearly half smaller than those of Kine cost and much smaller than those of Ener/Dyna costs. Repeated-measures

Table 3. Correlation analyses for RE and e3 indexes for all the participants. Correlation coefficients R , statistical significance p and slopes of linear regression (K) for two examined parameters (RE, e3) with respect to the peak of velocity (in m/s) are reported for each of the 15 subjects. Correlation coefficients significantly different from 0 are emphasized in bold

	S1	S2	S3	S4	S5	S6	S7	S8	S9	S10	S11	S12	S13	S14	S15
RE															
R	-0.63	-0.17	-0.12	-0.50	-0.76	-0.17	-0.26	-0.76	-0.62	-0.10	-0.43	-0.14	-0.05	0.10	0.06
p	$p < 0.001$	0.17	0.46	$p < 0.001$	$p < 0.001$	0.19	$p < 0.05$	$p < 0.001$	$p < 0.001$	0.49	$p < 0.01$	0.32	0.70	0.48	0.62
K_{RE}	-1.93	-0.82	-0.38	-2.60	-1.33	-0.51	-0.59	-1.98	-1.21	-1.61	-1.98	-0.69	-0.17	0.20	0.38
e3															
R	-0.61	-0.15	-0.46	-0.39	-0.85	0.02	0.14	-0.68	-0.88	-0.35	-0.48	-0.06	-0.21	0.10	0.20
p	$p < 0.001$	0.24	$p < 0.01$	$p < 0.01$	$p < 0.001$	0.82	0.27	$p < 0.001$	$p < 0.001$	$p < 0.05$	$p < 0.001$	0.65	0.11	0.50	0.12
K_{e3}	-1.21	-0.32	-0.80	-1.18	-1.53	0.08	0.22	-0.80	-1.3	-0.97	-0.87	-0.19	-0.41	0.13	0.93

ANOVAs indicated the significant differences in E_{Joint} between costs ($F(2.6,116.5) = 112.1, p < 0.001$). Post-hoc analysis revealed that the E_{Joint} of SDComp/SIComp were significantly smaller than those of three elementary costs but between the two composite costs there was no significant difference. Similar results were observed for E_{Cart} . The maximal deviations of simulated 3D finger paths from experimental ones were 5.1 ± 3.4 cm and 5.0 ± 3.2 cm for SDComp and SIComp respectively, while those of the three elementary costs were 8.9 ± 6.5 cm, 17.6 ± 9.2 , and 20.4 ± 4.5 cm for Kine, Ener and Dyna, respectively. Repeated-measures ANOVAs and Post-hoc analysis also showed significant differences in E_{Cart} between SDComp/SIComp and the three elementary costs but no significant differences between SDComp and SIComp. The chosen error was quite conservative given that it was based on maximal deviations. For the sake of comparison, the average deviation for the SIComp cost was 2.6 ± 2.0 cm, suggesting that average deviations were about half E_{Cart} in general. As such, this confirmed that the composite costs were significantly better to improve the goodness of fit by producing arm trajectories that matched quite accurately the recorded ones. Here, in order to visualize how well the simulated trajectories fit the empirical data, real and simulated arm trajectories using the uncovered speed-independent composite cost are plotted in Fig. 6.

Absolute and relative predictions of RE and e3 indexes across speeds. We quantified whether the identified composite costs could also replicate the movement parameters investigated above better than the elementary costs. The absolute reconstruction errors E_{RE} and E_{e3} for all examined costs are depicted in Fig. 7. In terms of E_{RE} (top left panel), a visual inspection revealed a quite large difference between the value of Dyna cost with respect to the others, thus implying that the reach endpoints predicted by such a dynamical criteria were quite far from the recorded ones regardless of the speed. For the other costs, the two composite costs SDComp/SIComp obtained relatively smaller values than Kine/Ener costs. Indeed, those values of these two costs were approximately three times smaller than those of Kine cost and five times smaller than those of Ener cost. Repeated-measures ANOVAs and Post-hoc analysis confirmed significant differences of E_{RE} between the two composite costs (SDComp/SIComp) and the three elementary costs (Kine/Ener/Dyna) ($F(2.8,121.5) = 81.3, p < 0.001$), but no significant difference between SDComp and SIComp ($p = 1.0$).

A similar analysis was carried out for e3 index (Fig. 7, bottom left panel). In agreement with the above results, a large difference for E_{e3} between Dyna cost and the others were still observed. Between composite costs (SDComp/SIComp) and the two elementary costs (Kine/Ener), the E_{e3} differences were smaller (approximately two third of the values for Kine/Ener costs). However, repeated-measures ANOVAs and Post-hoc analyses still indicated significant differences for E_{e3} between SDComp/SIComp and the three elementary costs ($F(2.2,95.9) = 17.7, p < 0.001$). Between the two

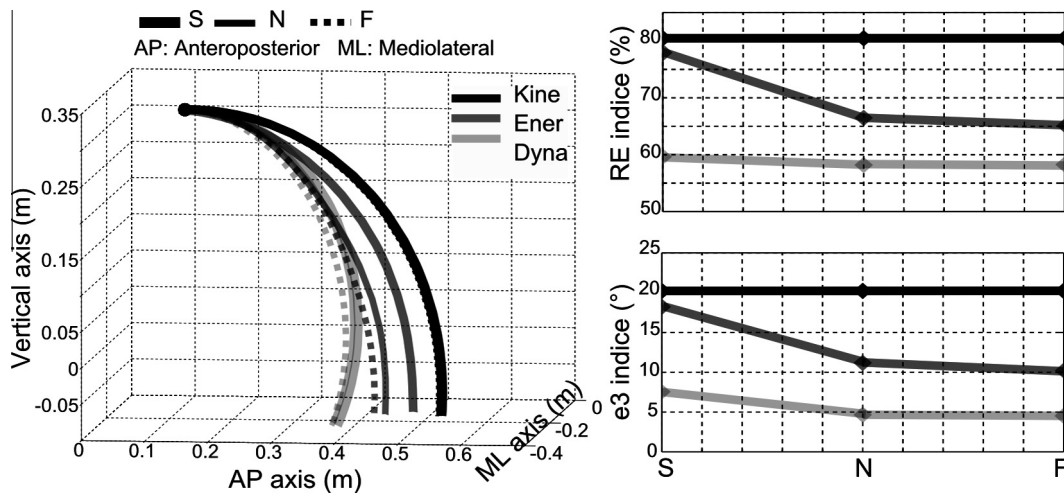


Fig. 4. Movement parameters predicted by each elementary cost (kinematic, energetic and dynamic) during the plane-reaching task at three different speeds (S, N and F). *Left.* Movement paths of the fingertip start from the same position (black circle) but end at different reach endpoints on the target surface. *Right.* Variation of RE and e3 indexes with respect to speed. The kinematic cost generated speed-invariant trajectories (constant movement path as well as RE and e3 indexes), whereas the dynamic and energetic costs generated relatively small and large speed-dependent trajectories respectively. RE and e3 indexes varied accordingly for the two latter costs. These two costs exhibited some degree of speed dependence because they both involved dynamic variables such as muscle torques and the musculoskeletal dynamics was highly nonlinear.

composite costs, no significant difference was observed ($p = 1.0$).

In order to assess whether costs could reproduce the speed-dependence (or independence) exhibited by each subject for e3 and RE indexes, the prediction of slopes given in Table 3 was investigated. The right panels in Fig. 7 shows the errors $E_{K_{RE}}$ and $E_{K_{e3}}$. In terms of RE index, it appeared that the Ener cost were quite large (about 2 times larger than Kine/Dyna and 3times larger than SDComp/SIComp), thus implying that the Ener cost tended to overestimate the speed-dependence of arm trajectories across subjects. Among the other costs tested, the Kine and Dyna costs obtained quite similar slope errors but these values were larger than those of SDComp/SIComp. Repeated-measures ANOVAs and Post-hoc analysis showed significant differences between the $E_{K_{RE}}$ of SDComp and Kine/Ener/Dyna ($F(2.4,33.8) = 4.7$, $p < 0.05$) but no significant difference between SDComp and SIComp ($p = 1.0$). Similar observations were obtained for $E_{K_{e3}}$. Repeated-measures ANOVAs and Post-hoc analysis showed a significant difference between SDComp/SIComp and Ener cost ($p < 0.05$). However, between SDComp/SIComp and Kine/Dyna, we did not observe any significant distinctions. Between SDComp and SIComp, again no significant difference was observed.

In summary, our results showed that only composite costs could reproduce both the absolute and speed-relative behaviors of the 15 participants. Furthermore, no significant gain was found when tuning the weights of the composite cost according motion speed compared to the assumption of a speed-independent composite cost. But if each subject relies upon an idiosyncratic composite cost function, a question remains about how to explain the emergence of speed-dependent and speed-independent arm trajectories. This issue is addressed hereafter.

Idiosyncrasy of composite costs. On average, composite costs were $\alpha_1 = 4.84 \times 10^3 \pm 3.15 \times 10^3$ and $\alpha_2 = 0.46 \times 10^2 \pm 0.43 \times 10^2$, but these weights varied across participants and appeared to be crucial to account for the arm trajectories across speeds. For instance, the coefficients characterizing the best-fitting composite cost for S5 was $\alpha = [1, 4.23 \times 10^3, 0.43 \times 10^2]$ and was $\alpha = [1, 2.71 \times 10^3, 0 \times 10^2]$ for S14. To get a more representative account of these costs, the contribution of each element was computed (see Materials and Methods). This analysis revealed that the Kine cost contributed on average across speeds and subjects to $80 \pm 15\%$ of the total cost while the Ener and Dyna costs were about $6 \pm 5\%$ and $13 \pm 12\%$ respectively. Although small, the previous analyses suggested that these contributions of energetic and dynamical costs were crucial to replicate the speed-dependences observed several subjects. Yet, although they used a composite cost, some other subjects did not exhibit speed-dependent behaviors.

To better understand the role of the weights onto the speed-dependence of arm trajectories for each subject, we varied the energetic (α_1) and dynamic (α_2) coefficients of the composite cost ($C(\alpha) = C_{Kine} + \alpha_1 C_{Ener} + \alpha_2 C_{Dyna}$) and evaluated the speed-dependence of trajectories predicted from forward optimal control simulations. The resulting slopes K_{RE} , K_{e3} and joint space fitting error E_{Joint} (the minimized quantity during inverse optimal control) for the two subjects S5 (*left*) and S14 (*right*) were computed and depicted in Fig. 8. It is noteworthy that these two subjects had different anthropometric parameters, thus allowing to test whether anthropometric discrepancies could explain differences in speed sensitivity at fixed composite cost. For both subjects, the patterns of K_{RE} and K_{e3} were relatively similar but the speed-dependence of S5 appeared to be much larger in terms of magnitudes.

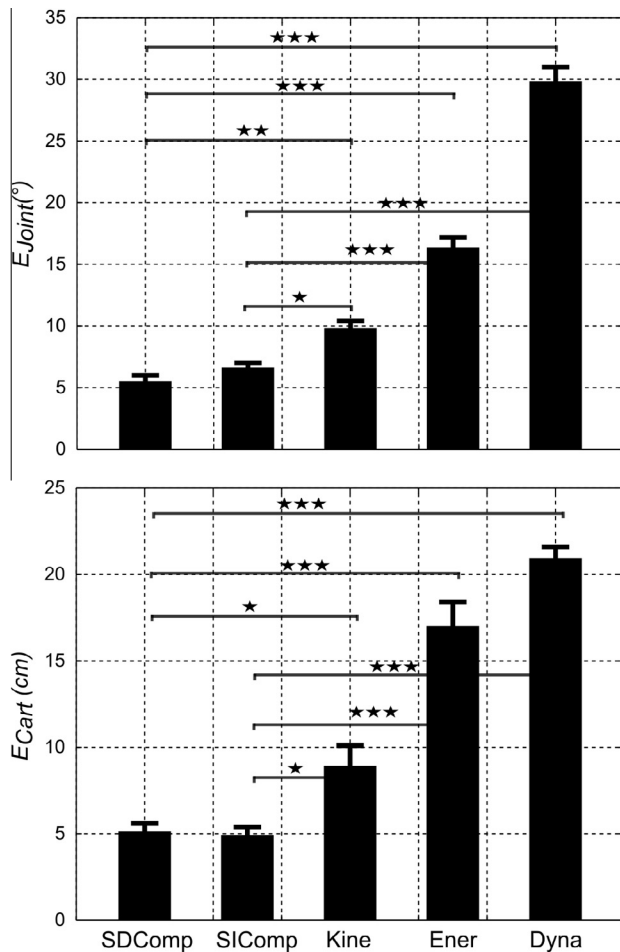


Fig. 5. Reconstruction errors in joint space (E_{Joint}) and Cartesian space (E_{Cart}) for the best-fitting speed-dependent composite cost (SDComp) and speed-independent composite cost (SIComp) as well as each of the three cost elements taken separately, for the different speeds (S, N and F). Error values were averaged across subjects (with standard errors indicated by error bars). Noticeably, in terms of both joint and Cartesian errors, the composite costs (SDComp and SIComp) performed better than each elementary cost taken alone (Kine, Ener and Dyna). Horizontal bars with stars indicate the results of post-hoc analysis. One, two and three stars stand for $p < 0.05$, $p < 0.01$ and $p < 0.001$ respectively.

This implied that if both subjects had used the same composite cost, S5 would intrinsically appear to be more speed-dependent than S14 just because of anthropometric peculiarities. On the other hand, by changing the weights of the composite cost, subject S5 had the possibility to be more or less speed-dependent. Similarly, subject S14 could be speed-dependent if increasing the weights of the energy and dynamic coefficients. Nevertheless, this would have changed their arm trajectories (and the minimum in E_{Joint} graphs) and this is why it was not found by the inverse optimal control algorithm in the present data.

In summary, these 3D plots show that anthropometry partly explains why a given composite costs may lead to differences in terms of speed dependence of behaviors. However, the composition of composite costs was clearly idiosyncratic, thereby implying that different arm

trajectories also emerged across subjects because of differences in the weighting of kinematic, energetic and dynamic variables.

DISCUSSION

In this work, we examined the nature of motor planning variables during free-endpoint arm reaching task. Three-dimensional arm movements without a prescribed reach endpoint location were investigated and how speed instructions affected the chosen arm trajectories was measured. The experimental results showed that the reach endpoint (RE) and rotation axis displacements (e3/SE) significantly varied with speed to an extent that depended on individual factors. These idiosyncratic behaviors were accounted for in the framework of optimal control as the outcome of the minimization of a cost weighting kinematic, energetic and dynamic variables. The latter quantities were assumed to represent (a priori) internal values guiding motor decision within the brain and were essentially found to be subject-specific but speed independent. These results are discussed in more detail hereafter.

Unrestrained 3D arm trajectories: speed dependence or independence

Our findings revealed significant speed-related changes in both arm trajectories during the free 3D arm movements under consideration, which contrasts with classical conclusions drawn in point-to-point movement studies. Whether the brain controls movement using speed-sensitive or speed-insensitive planning strategies is a long-standing issue in motor control. The term speed-insensitive is used when prominent aspects of the motor strategy (e.g. hand path, time-course of velocity or acceleration) remain invariant in spite of speed differences and/or when simple scaling rules apply to the motor patterns. This question has been extensively investigated for horizontal or vertical planar point-to-point 2D movements (Soechting and Lacquaniti, 1981; Atkeson and Hollerbach, 1985; Flash and Hogan, 1985; Ostry et al., 1987; Gordon et al., 1994; Soechting et al., 1995; Flanders et al., 1996). In those seminal studies, hand paths were generally considered as straight or slightly curved and velocity profiles bell-shaped regardless of motion speed, as if a scaling law applied to a unique movement pattern. Finer analyses however revealed that the timing of velocity profiles was significantly affected by the speed at which movements were executed (Nagasaki, 1989; Papaxanthis et al., 1998, 2003), in agreement with the well-known fact that deceleration duration increases when maximal accuracy and speed are together required, such as in Fitts-like experiments (Woodworth, 1899; Fitts, 1954; MacKenzie and Iberall, 1994; Elliott et al., 2001). Even in those such settings, however, the shape of hand paths was widely accepted to be speed-invariant. Further studies extended planar point-to-point reaching paradigms to the 3D case to better tackle the speed-dependence question and lead to the conclusion that, given an initial arm posture and a final target position, neither the final arm posture nor the

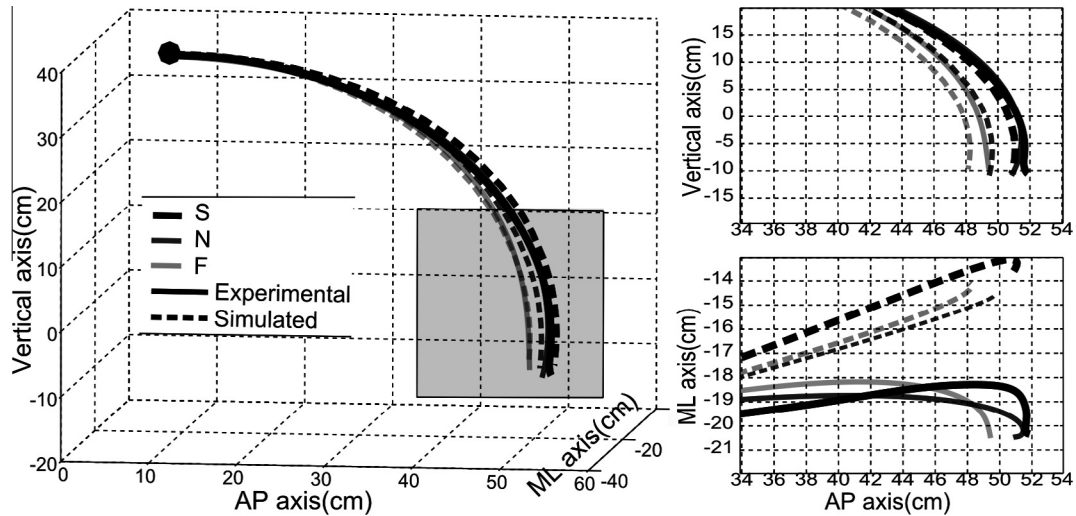


Fig. 6. Simulated finger paths predicted from the best-fitting composite cost (SIComp) and average experimental finger paths for subject S5. *Left.* 3D finger paths for the three speeds for experimental (plain traces) and simulated (dotted lines) data. *Right.* The zoomed-in projections of finger paths on the sagittal plane (*top*) and the transverse plane (*bottom*) for the last part of the movement, in order to emphasize differences. In general, fitting errors mainly arose from the discrepancy of trajectories along the ML axis while along the AP axis (main axis of interest here), the simulated trajectories better matched the recorded ones and clearly exhibited a speed dependence.

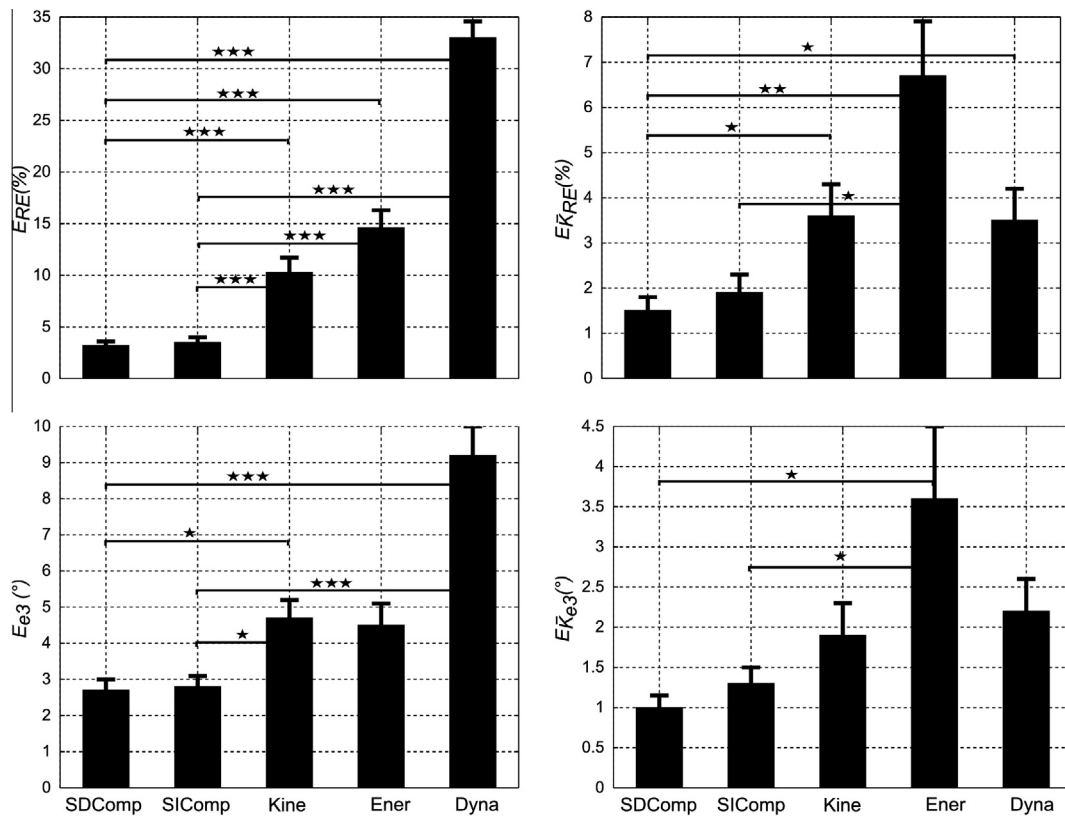


Fig. 7. Reconstruction errors for some relevant movement parameters (E_{e3} , E_{RE} , E_{KRE} , E_{KRE3}) for the SDComp, SIComp costs and the three cost elements taken separately. Error values were first averaged across speeds and then across subjects (with standard errors indicated by error bars). Visual inspection reveals that in terms of both E_{RE} and E_{e3} the dynamic cost performs quite poorly compared to the other costs. In terms of E_{KRE} and E_{KRE3} , the energy cost overestimates the speed dependence of RE and e3 parameters. Overall, the kinematic cost performs relatively well but the composite costs perform significantly better than the latter. Importantly, the kinematic cost is also unable to account for any speed-dependence as it predicts constant movement parameters for all speeds. Finally, no significant difference was found between the SDComp and SIComp.

hand path curvature depended significantly on movement speed (Nishikawa et al., 1999; Zhang and Chaffin, 1999). This lack of significant differences may have been due to

the specification of a precise target to reach to, which could have limited the expression or the finding of speed-dependent arm trajectories. Indeed our protocol

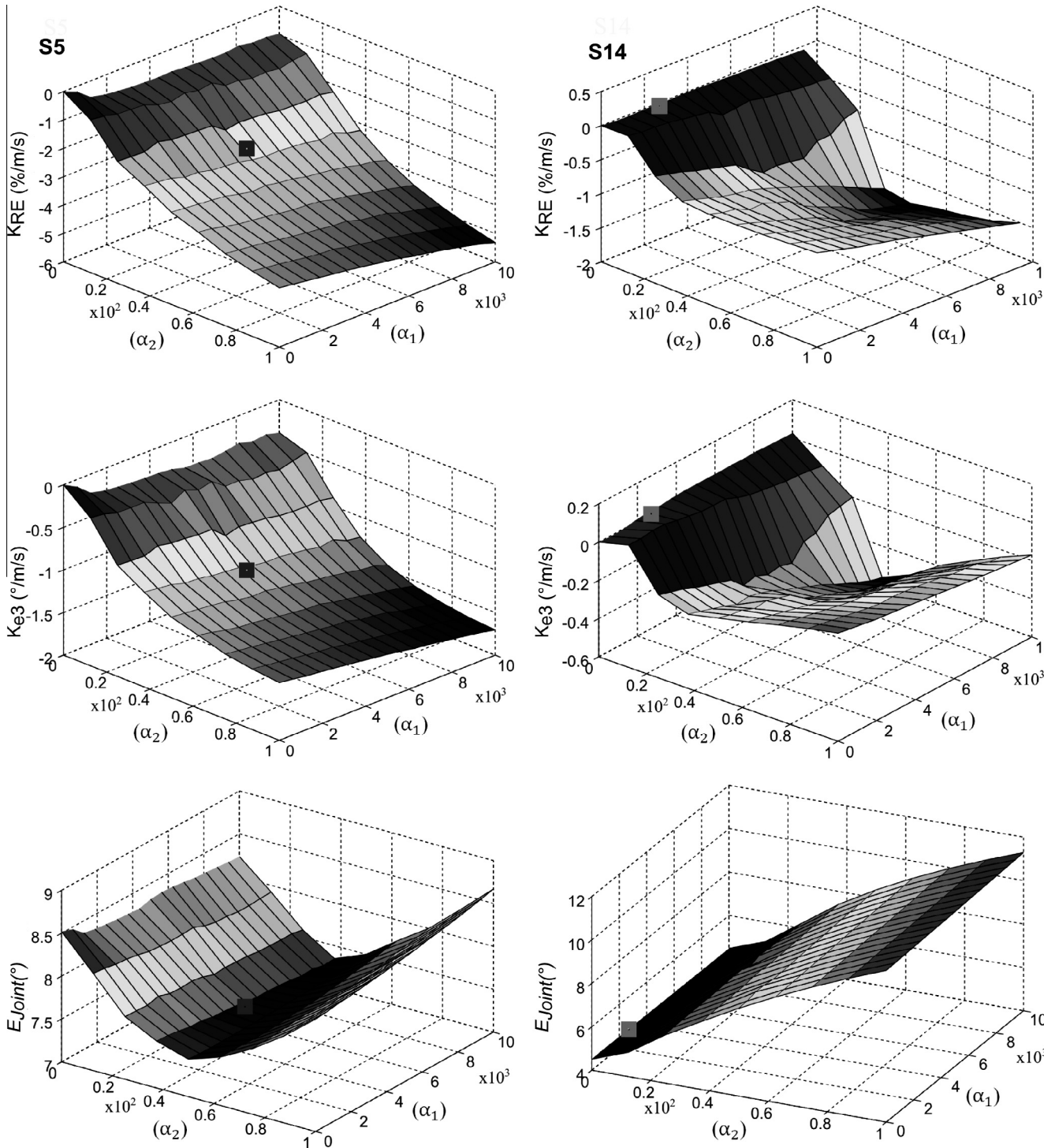


Fig. 8. 3D plots of K_{RE} , K_{e3} and E_{Joint} for the two typical subjects S5 (left) and S14 (right) as a function of the weights of the composite cost $C(\alpha)$. In these graphs, α_1 and α_2 were varied to visualize how the speed dependence as well as the error minimized during inverse optimal control varied according to the chosen weights. Remind that $C(\alpha) = C_{Kine} + \alpha_1 C_{Ener} + \alpha_2 C_{Dyna}$. The squares indicated on each 3D plot show the position of the best-fitting speed-independent composite cost (SIComp) found during inverse optimal control. S5 and S14 have different anthropometric characteristics. Interestingly, by choosing appropriate α_1 and α_2 weights, subjects could exhibit different degree of speed dependence (almost zero K_{RE}/K_{e3} or negative K_{RE}/K_{e3}). For example, S14 could have been speed dependent if he/she chose a different cost combination (but this was not uncovered here because his/her trajectories were not compatible with such a cost function).

defined looser task constraints in terms of the final hand position, which may be the reason why the reach endpoint as well as certain joint displacements depended significantly on the motion speed. Dealing with tasks involving

undefined reach endpoints is nevertheless ecological and occurs in many tasks. For example catching a ball (e.g. Cesqui et al., 2012) is a task involving an infinity of possible reach endpoints along the ball's trajectory. The

existence of differences between constrained and unconstrained tasks was already noticed in [Desmurget et al. \(1997\)](#). The speed dependence found here for discrete movements is also consistent with what [Isableu et al. \(2009\)](#) observed during a cyclical yet comparable arm movement task in which a similar speed-dependent tuning of motor strategy was observed for some subjects. To account for the experimental arm trajectories, we had recourse to inverse optimal control as it makes hypotheses about the nature of the variables possibly relevant to motor planning.

Motor planning variables: kinematic, energetic, dynamic or composite

The above issue about the speed dependence of motor strategies is actually tightly linked with the nature of hypothetical cost functions involved in motor planning, as already noticed in [Soechting and Flanders \(1998\)](#). The former problem actually gains at being rephrased within the normative framework of optimal control as it simplifies both its formulation and analysis. Indeed, analyzing the subjects' behavior in terms of cost functions instead of a bunch of 3D arm trajectories can be seen as a dimensionality reduction since a cost function summarizes the spatiotemporal characteristics of an infinity of joint trajectories at once (see [Berniker and Kording, 2015](#)). In the optimal control context, the issue of kinematic versus dynamic motor planning has been the topic of several investigations ([Flanagan and Rao, 1995](#); [Soechting et al., 1995](#); [Wolpert et al., 1995](#); [Soechting and Flanders, 1998](#); [Vetter et al., 2002](#); [Hermens and Gielen, 2004](#)). Here, solely optimizing an energetic or a dynamic criterion was not adequate for replicating the basic features of arm trajectories: the reach endpoints and the final postures were just too discrepant with the data (see [Fig. 7](#)). In contrast, optimizing a kinematic cost performed quite well at a first sight. Accordingly, it was found to be the primary cost accounting for the arm displacement of subjects and the dominant humeral rotations. Rotations around the humeral axis (i.e. SE axis) were interpreted in [Soechting et al. \(1995\)](#) as cues of a planning of energetically efficient arm trajectories but the present task shows that strictly rotating around the humeral axis was not energetically optimal (at least when energy expenditure is measured by the absolute work of muscle torques and not as the peak of positive work as in [Soechting et al. \(1995\)](#)). The kinematic cost was however not appropriate if one considers the speed-dependence of behaviors. Indeed, such a kinematic cost predicts invariant patterns of joint trajectories when speed varies. Hence, speed does not affect hand path in such models, which was not compatible with the behavior of most participants. From a computational standpoint, kinematic models may be appealing as they do not require new inverse internal model to extract adequate motor commands matching a wide range of velocities. Indeed, taking gravitational and frictional torques apart, the structure of rigid body dynamics is such that movements of different speeds can be generated from a single torque pattern τ despite the non-linearity of the arm dynamics by means of a simple scaling law of the type

$\tilde{\tau}(t) = r^2\tau(rt)$ (see [Hollerbach and Flash, 1982](#) for details). More generally, any strategy relying on such a spatiotemporal rescaling of a reference torque pattern (be it initially based upon kinematic, kinetic or any composite optimality criteria) would yield the same hand paths and final postures. Even though experimental evidence was provided for a separation between tonic versus speed-related phasic muscle activity during point-to-point motor tasks ([Flanders and Herrmann, 1992](#); [Flanders et al., 1996](#)), the fact that the reach endpoints or other parameters depended significantly upon speed in our data made impossible such a basic scaling principle. The systematic and consistent speed-dependent changes of arm trajectories observed in the present study rather supported the existence of a composite cost underlying the formation of arm trajectories for the range of speeds under consideration. Furthermore, geometric models such as the geodesic model ([Biess et al., 2007](#)) would not be able to account for these experimental findings as they hypothesize a decoupling between the geometric and temporal properties of movement, which is at odds with our experimental findings. Therefore, taken together, our findings revealed the composite nature of the cost function underlying arm movement. These findings extended those found for planar motion in [Berret et al. \(2011b\)](#). Other studies using a different motor task (landing after a vertical jump) reached very similar conclusions about the combination of energetic/dynamic criteria with other factors such as comfort or smoothness ([Zelik and Kuo, 2012](#); [Skinner et al., 2015](#)).

Flexibility of the composite optimality criterion

Within the theory of composite cost functions, there exist intriguing questions pertaining to the degree of flexibility of the combinations. In particular, whether speed affects or not the way elementary costs are weighted was an open question. If results indicate that kinematic, energetic and dynamic costs must be combined to fit the data to the greatest possible extent, the relative relevance of each of these quantities may differ as their order of magnitude also vary with speed. It could be possible that at large speeds, limiting angular jerk because more important than minimizing energy expenditure. In [Berret et al. \(2011b\)](#), arm trajectories starting from several initial postures were studied and a single composite cost was assumed to account for movements starting from all positions at once. However, the study only considered a single movement pace, namely a quick speed. Thus, whether a single combination of costs would also be valid for movements performed at various speeds was uncertain even though, within the composite cost hypothesis, understanding the extent to which the weights depend on external or internal factors seems crucial. The question is also relevant when attempting to predict the pace of natural movements ([Shadmehr, 2010](#); [Shadmehr et al., 2010](#); [Berret and Jean, 2016](#)). In these works, a cost of time was assumed to be combined with trajectory costs (i.e. the subjective costs studied here) and other objective costs. How speed instructions affect such mixtures of costs is not clear especially if the exact nature of the trajectory costs changes with speed instructions. When

instructed a subject to move fast or slow, which weights are exactly modified is hard to identify in general. Here we addressed this problem (without considering the cost of time as it does not matter when movement time is taken directly from experimental data as we did here) and assessed whether the weights depended or not on the instructed speed. Our results supported the fact that the speed dependence of arm trajectories of each participant could be accounted for by a unique composite cost (i.e. with invariant weights). Indeed, no significant gain was found when tuning the weights according to the instructed speed. This is especially if one considers the addition of new fitting parameters when doing so. Following Occam's razor principle, we could not retain the more complex model consisting of adjusting the weights according to movement speed. While we cannot exclude that the weights of objective costs such as accuracy or precision did not change when speed increased because we did not model sensorimotor noise, our conclusions only concern the subjective optimality criterion. Simulations conducted within the stochastic optimal control framework would be required to address such questions (Todrov, 2006), but the numerical tools are not as advanced as in the deterministic settings and therefore treating the stochastic case was not considered. We cannot exclude neither the existence of other subjective costs (there is infinity of movement-related costs and other costs less quantifiable such as discomfort, pain, gracefulness etc.) but the present findings nonetheless argued for a subject-specific composite nature of motor planning variables. It could still be argued that the participants exhibiting the strongest speed dependences of arm trajectories simply suffered from inaccurate sensorimotor control, which would just be emphasized at large speeds. However, the consistency of speed-related fluctuations across trials for these participants tends to disagree with this hypothesis. Moreover, the CNS is known to have good capabilities to predict and anticipate interaction torques (Gribble and Ostry, 1999) and the inertial anisotropy of the human arm (Gordon et al., 1994; van Beers et al., 2004) during motor planning as well as gravity (Berret et al., 2008; Gaveau et al., 2011, 2014). Therefore, rather than interpreting their behaviors as the realization of inefficient motor control, we instead interpret them as the outcome of efficient motor control, which may be the signature of a composite cost proper to each individual.

Inter-individual differences

Interesting inter-individual differences were pointed out throughout the study, especially with respect to speed instruction. Motivated by applications in neuro-rehabilitation, neuro-prosthetics and related areas, the study of inter-individual differences has developed as a hot topic of research in recent years. Many researchers tried to find whether idiosyncrasy arises from a peripheral or central origin and tried to elaborate on principles that could account for them. In this vein, initial assumptions were related to a different involvement and exploitation of frames of reference (e.g. visual versus kinesthetic) and to changes from one frame of reference

to another with respect to execution speed (Pozzo et al., 1991; Isableu et al., 2003; Bernardin et al., 2005). Recently, Isableu et al. (2009) provided evidence of individual differences in a task where cyclical 3D arm movements were experimented. These authors showed that different subjects moved preferentially around different rotation axes: some participants always rotated their arm around the geometrical articular axis (termed as "kinematicians") or around the minimum inertia axis regardless of speed (termed as "dynamicians") while other switched from the geometrical to the minimum inertia axis when movement speed increased. It was proposed that these rotational axis preferences could originate from prior sensorimotor strategies experienced by the subjects. These strategies indeed allowed subjects to differentially exploit the dynamical arm properties and the passive torques (e.g. interaction or gravity torques) in order to minimize the inertial resistance as well as the muscle torque input to the movement. It is however hard to separate differences due to anthropomorphic or peripheral specificity from those arising from different motor planning principles. The current results thus extend these previous findings for a discrete task and refined them within the context of optimal control. In particular, our results further showed that the subject-specific motor strategies actually correspond to different subjective composite costs. In fact, optimal control simulations take into account the anthropometric characteristics of each participant and if differences between subjects could be explained by such body-related peculiarities then the same composite cost function would have been identified using inverse optimal control. Since different subjects appeared to weight very differently the cost elements, our results rather argue in favor of divergences in the central representation of movement and the subjective values actually attributed to the motor task (smoothness, mechanical energy, muscle torques...). The importance of individual factors when the task constraints are loose, as during such a free-endpoint reaching task, was already pointed out by Cesqui et al. (2012) in a ball catching task. In this task, equally successful yet very different motor solutions were adopted by subjects. We showed that such different solutions were not fully due to musculoskeletal discrepancies across participants but may rather reflect different subjective costs that can operate vicariously. More precisely here our results revealed that the subjects who presented relatively invariant trajectories generally relied upon a kinematic objective or a combination of kinematic and a small amount of energetic objectives regardless of speed (Fig. 8), while other participants who presented a change of trajectories often relied upon a combination of kinematic, energetic and dynamic objectives. Depending on the composite cost chosen, varying the anthropometric characteristics could change the degree of speed-dependence of an individual. On the other hand, for fixed anthropometric characteristics, the relative weights defining the composite cost were critical to explain the degree of speed-dependence of each participant, which proved that inter-individual differences were not only due to anthropometric divergences but also to central factors. These factors may be encoded and

traded-off through the cortex-basal ganglia network (e.g. Scott, 2004; Turner and Desmurget, 2010 for reviews) where these variables shaping arm movement trajectories would be valued and might guide motor planning in terms of objective and subjective costs or rewards.

Research limitations

One could wonder whether the reconstruction errors we obtained are small enough to conclude that the composite cost really constitutes a high-level representation of motor planning objectives. It is indeed undeniable that there might still exist a more universal cost accounting better for the present experimental data. Finding such a ubiquitous cost function would be appealing for motor control but what would be its nature and shape is still an open question. Thus far, the existing literature has reported the relevance of several cost functions in the exact same way that neurophysiological studies have reported cortical representation of a large variety of movement-related parameters ranging from kinematic (spatial or nonspatial) to dynamic or muscular. Therefore, assuming composite cost functions is a solution compatible with previous findings that may moreover reconcile prior computational and empirical studies. Within this composite cost hypothesis, knowing which elementary cost should be included may nevertheless be tricky as candidate costs are numerous. The situation is even more complex with regards to the number of DoFs of the system. Precisely, any cost such as the angle jerk is intrinsically composite since different weights could be attributed to different DoFs. In general, researchers have assumed that all those weights are equal to one (including in the present study) for the sake of simplicity but one can easily imagine that such weights actually vary across DoFs. Throughout our analyses, we thus conducted supplementary tests to evaluate whether reconstruction error could be improved by (i) adding other elementary costs or (ii) tuning the weights of the kinematic, energetic and dynamic costs for each DoF separately. To test (i) we added costs such as acceleration, geodesic and muscle torque as in Berret et al. (2011b). In this case, the best-fitting speed-independent composite cost yielded maximal Cartesian deviations (i.e. E_{Cart} values) of 4.3 ± 2.6 cm, which is not much smaller than when dealing with three costs as we did in our study. Hence the three costs we retained in the current study were quite relevant to account for the present data. This was confirmed when looking at (ii). When we allowed optimization of the weights associated to each DoF separately we found E_{Cart} values of 3.1 ± 2.1 cm. Compared to the 5 cm in our main results, the improvement seems notable even though this approach required 11 variables to be adjusted during the inverse optimal control process (instead of 2 otherwise). This finding suggests that a fine tuning of the weight at each DoF would allow a better replication of the real arm trajectories. However, this approach would drastically complicate the analysis unless one groups the weights according to the underlying type of cost, i.e. kinematic, energetic and dynamic, as we eventually did

here. As such, these considerations show that our main conclusions about the compositeness and speed-dependence of optimality criteria would not differ if choosing slightly different modeling approaches.

REFERENCES

- Asfour T, Dillmann R (2003) Human-like motion of a humanoid robot arm based on a closed-form solution of the inverse kinematics problem In *Intelligent Robots and Systems*, 2003. (IROS 2003). In: *Proceedings. 2003 IEEE/RSJ International Conference on*, Vol. 2. p. 1407–1412.
- Atkeson CG, Hollerbach JM (1985) Kinematic features of unrestrained vertical arm movements. *J Neurosci* 5:2318–2330.
- Bastian AJ, Martin TA, Keating JG, Thach WT (1996) Cerebellar ataxia: abnormal control of interaction torques across multiple joints. *J Neurophysiol* 76:492–509.
- Ben-Itzhak S, Karniel A (2008) Minimum acceleration criterion with constraints implies bang-bang control as an underlying principle for optimal trajectories of arm reaching movements. *Neural Comput* 20(3):779–812.
- Bernardin D, Isableu B, Fourcade P, Bardy BG (2005) Differential exploitation of the inertia tensor in multi-joint arm reaching. *Exp Brain Res* 167:487–495.
- Berniker M, Kording KP (2015) Deep networks for motor control functions. *Front Comput Neurosci* 9:32.
- Berret B, Darlot C, Jean F, Pozzo T, Papaxanthis C, Gauthier JP (2008) The inactivation principle: mathematical solutions minimizing the absolute work and biological implications for the planning of arm movements. *PLoS Comput Biol* 4:e1000194.
- Berret B, Jean F (2016) Why don't we move slower? The value of time in the neural control of action. *J Neurosci* 36(4):1056–1070.
- Berret B, Bisio A, Jacono M, Pozzo T (2014) Reach endpoint formation during the visuomotor planning of free arm pointing. *Eur J Neurosci* 40:3491–3503.
- Berret B, Chiovetto E, Nori F, Pozzo T (2011a) Evidence for composite cost functions in arm movement planning: an inverse optimal control approach. *PLoS Comput Biol* 7:e1002183.
- Berret B, Chiovetto E, Nori F, Pozzo T (2011b) Manifold reaching paradigm: how do we handle target redundancy? *J Neurophysiol* 106:2086–2102.
- Biess A, Liebermann DG, Flash T (2007) A computational model for redundant human three-dimensional pointing movements: integration of independent spatial and temporal motor plans simplifies movement dynamics. *J Neurosci* 27:13045–13064.
- Cesqui B, d'Avella A, Portone A, Lacquaniti F (2012) Catching a ball at the right time and place: individual factors matter. *PLoS One* 7:e31770.
- Darling WG, Hondzinski JM (1999) Kinesthetic perceptions of earth- and body-fixed axes. *Exp Brain Res* 126:417–430.
- Debicki DB, Gribble PL, Watts S, Hore J (2011) Wrist muscle activation, interaction torque and mechanical properties in unskilled throws of different speeds. *Exp Brain Res* 208:115–125.
- Debicki DB, Watts S, Gribble PL, Hore J (2010) A novel shoulder–elbow mechanism for increasing speed in a multijoint arm movement. *Exp Brain Res* 203:601–613.
- Desmurget M, Jordan M, Prablanc C, Jeannerod M (1997) Constrained and unconstrained movements involve different control strategies. *J Neurophysiol* 77:1644–1650.
- Dounskaia NV, Ketcham CJ, Stelmach GE (2002) Influence of biomechanical constraints on horizontal arm movements. *Motor Control* 6:366–387.
- Dumas R, Chèze L, Verriest JP, et al. (2007) Adjustments to McConville et al. and young et al. body segment inertial parameters. *J Biomech* 40:543–553.
- Elliott D, Helsen WF, Chua R (2001) A century later: Woodworth's (1899) two-component model of goal-directed aiming. *Psychol Bull* 127:342–357.

- Featherstone R, Orin D (2000) Robot dynamics: equations and algorithms In *Robotics and Automation, 2000*. In: Proceedings. ICRA'00. IEEE International Conference on, Vol. 1. p. 826–834.
- Fitts PM (1954) The information capacity of the human motor system in controlling the amplitude of movement. *J Exp Psychol* 47:381–391.
- Flanagan JR, Rao AK (1995) Trajectory adaptation to a nonlinear visuomotor transformation: evidence of motion planning in visually perceived space. *J Neurophysiol* 74:2174–2178.
- Flanders M, Herrmann U (1992) Two components of muscle activation: scaling with the speed of arm movement. *J Neurophysiol* 67:931–943.
- Flanders M, Pellegrini JJ, Geisler SD (1996) Basic features of phasic activation for reaching in vertical planes. *Exp Brain Res* 110:67–79.
- Flash T, Hogan N (1985) The coordination of arm movements: an experimentally confirmed mathematical model. *J Neurosci* 5:1688–1703.
- Galloway JC, Koshland GF (2002) General coordination of shoulder, elbow and wrist dynamics during multijoint arm movements. *Exp Brain Res* 142:163–180.
- Gauthier JP, Berret B, Jean F (2010) A biomechanical inactivation principle. *Proceedings of the Steklov Institute of Mathematics* 268:93–116.
- Gaveau J, Paizis C, Berret B, Pozzo T, Papaxanthis C (2011) Sensorimotor adaptation of point-to-point arm movements after spaceflight: the role of internal representation of gravity force in trajectory planning. *J Neurophysiol* 106:620–629.
- Gaveau J, Berret B, Demougeot L, Fadiga L, Pozzo T, Papaxanthis C (2014) Energy-related optimal control accounts for gravitational load: comparing shoulder, elbow, and wrist rotations. *J Neurophysiol* 111:4–16.
- Georgopoulos AP, Kalaska JF, Caminiti R, Massey JT (1982) On the relations between the direction of two-dimensional arm movements and cell discharge in primate motor cortex. *J Neurosci* 2:1527–1537.
- Gielen S (2009) Review of models for the generation of multi-joint movements in 3-D. In: *Progress in Motor Control. A Multidisciplinary Perspective*. US: Springer. p. 523–550.
- Gordon J, Ghilardi MF, Cooper SE, Ghez C (1994) Accuracy of planar reaching movements. ii. systematic extent errors resulting from inertial anisotropy. *Exp Brain Res* 99:112–130.
- Gribble PL, Ostry DJ (1999) Compensation for interaction torques during single- and multijoint limb movement. *J Neurophysiol* 82:2310–2326.
- Gribble PL, Ostry DJ, Sanguineti V, Laboisière R (1998) Are complex control signals required for human arm movement? *J Neurophysiol* 79:1409–1424.
- Guigon E, Baraduc P, Desmurget M (2007) Computational motor control: redundancy and invariance. *J Neurophysiol* 97:331–347.
- Hermens F, Gielen S (2004) Posture-based or trajectory-based movement planning: a comparison of direct and indirect pointing movements. *Exp Brain Res* 159:340–348.
- Hirashima M, Kudo K, Watarai K, Ohtsuki T (2007) Control of 3d limb dynamics in unconstrained overarm throws of different speeds performed by skilled baseball players. *J Neurophysiol* 97:680–691.
- Hollerbach MJ, Flash T (1982) Dynamic interactions between limb segments during planar arm movement. *Biol Cybern* 44:67–77.
- Hore J, Debicki DB, Watts S (2005) Braking of elbow extension in fast overarm throws made by skilled and unskilled subjects. *Exp Brain Res* 164:365–375.
- Hore J, Debicki DB, Gribble PL, Watts S (2011) Deliberate utilization of interaction torques brakes elbow extension in a fast throwing motion. *Exp Brain Res* 211:63–72.
- Isableu B, Rezzoug N, Mallet G, Bernardin D, Gorce P, Pagano CC (2009) Velocity-dependent changes of rotational axes in the non-visual control of unconstrained 3d arm motions. *Neuroscience* 164:1632–1647.
- Isableu B, Ohlmann T, Crémieux J, Amblard B (2003) Differential approach to strategies of segmental stabilisation in postural control. *Exp Brain Res* 150:208–221.
- Kalaska JF, Cohen DA, Hyde ML, Prud'homme M (1989) A comparison of movement direction-related versus load direction-related activity in primate motor cortex, using a two-dimensional reaching task. *J Neurosci* 9:2080–2102.
- Kawato M, Furukawa K, Suzuki R (1987) A hierarchical neural-network model for control and learning of voluntary movement. *Biol Cybern* 57:169–185.
- Knill DC, Bondada A, Chhabra M (2011) Flexible, task-dependent use of sensory feedback to control hand movements. *J Neurosci* 31:1219–1237.
- MacKenzie C, Iberall T (1994) *The Grasping Hand Advances in psychology*. North-Holland.
- Mombaur K, Truong A, Laumond JP (2009) From human to humanoid locomotion - an inverse optimal control approach. *Autonomous Robots*.
- Mussa-Ivaldi FA (1988) Do neurons in the motor cortex encode movement direction? an alternative hypothesis. *Neurosci Lett* 91:106–111.
- Nagasaki H (1989) Asymmetric velocity and acceleration profiles of human arm movements. *Exp Brain Res* 74:319–326.
- Nakano E, Imamizu H, Osu R, Uno Y, Gomi H, Yoshioka T, Kawato M (1999) Quantitative examinations of internal representations for arm trajectory planning: minimum commanded torque change model. *J Neurophysiol* 81:2140–2155.
- Nelson WL (1983) Physical principles for economies of skilled movements. *Biol Cybern* 46:135–147.
- Nishii J, Murakami T (2002) Energetic optimality of arm trajectory. In: *Proc of Int Conf on Biomechanics of Man*. p. 30–33.
- Nishikawa KC, Murray ST, Flanders M (1999) Do arm postures vary with the speed of reaching? *J Neurophysiol* 81:2582–2586.
- Ostry DJ, Cooke JD, Munhall KG (1987) Velocity curves of human arm and speech movements. *Exp Brain Res* 68:37–46.
- Pagano CC, Turvey MT (1995) The inertia tensor as a basis for the perception of limb orientation. *J Exp Psychol Hum Percept Perform* 21:1070–1087.
- Papaxanthis C, Pozzo T, Schieppati M (2003) Trajectories of arm pointing movements on the sagittal plane vary with both direction and speed. *Exp Brain Res* 148:498–503.
- Papaxanthis C, Pozzo T, Stapley P (1998) Effects of movement direction upon kinematic characteristics of vertical arm pointing movements in man. *Neurosci Lett* 253:103–106.
- Pozzo T, Berthoz A, Lefort L, Vitte E (1991) Head stabilization during various locomotor tasks in humans. ii. patients with bilateral peripheral vestibular deficits. *Exp Brain Res* 85:208–217.
- Rao AV, Benson DA, Darby CL, Patterson MA, Francolin C, Sanders I, Huntington GT (2010) Algorithm 902: Gpops, a matlab software for solving multiple-phase optimal control problems using the gauss pseudospectral method. *ACM Transactions on Mathematical Software* 37:1–39.
- Riley MA, Turvey MT (2001) Inertial constraints on limb proprioception are independent of visual calibration. *J Exp Psychol Hum Percept Perform* 27:438–455.
- Sainburg RL, Ghez C, Kalakanis D (1999) Intersegmental dynamics are controlled by sequential anticipatory, error correction, and postural mechanisms. *J Neurophysiol* 81:1045–1056.
- Sainburg RL, Ghilardi MF, Poizner H, Ghez C (1995) Control of limb dynamics in normal subjects and patients without proprioception. *J Neurophysiol* 73:820–835.
- Sainburg RL, Kalakanis D (2000) Differences in control of limb dynamics during dominant and nondominant arm reaching. *J Neurophysiol* 83:2661–2675.
- Sande de Souza LAP, Dioísio VC, Lerena MAM, Marconi NF, Almeida GL (2009) The linear co-variance between joint muscle torques is not a generalized principle. *J Electromyogr Kinesiol* 19: e171–e179.
- Scott SH (2004) Optimal feedback control and the neural basis of volitional motor control. *Nat Rev Neurosci* 5:532–546.

- Shadmehr R (2010) Control of movements and temporal discounting of reward. *Curr Opin Neurobiol* 20:726–730.
- Shadmehr R, Orban de Xivry JJ, Xu-Wilson M, Shih TY (2010) Temporal discounting of reward and the cost of time in motor control. *J Neurosci* 30:10507–10516.
- Skinner NE, Zelik KE, Kuo AD (2015) Subjective valuation of cushioning in a human drop landing task as quantified by trade-offs in mechanical work. *J Biomech* 48:1887–1892.
- Soechting JF, Buneo CA, Herrmann U, Flanders M (1995) Moving effortlessly in three dimensions: does Donders' law apply to arm movement? *J Neurosci* 15:6271–6280.
- Soechting JF, Flanders M (1998) Movement planning: kinematics, dynamics, both or neither? *Vision and Action*. In: Harris LR, Jenkin M, editors. Cambridge, UK: Cambridge Univ. Press.
- Soechting JF, Lacquaniti F (1981) Invariant characteristics of a pointing movement in man. *J Neurosci* 1:710–720.
- Todorov E (2004) Optimality principles in sensorimotor control. *Nat Neurosci* 7:907–915.
- Todorov E (2006) Optimal control theory. In: Doya K, editor. *Bayesian Brain: Probabilistic Approaches to Neural Coding*. p. 269–298 (chapter 12).
- Turner RS, Desmurget M (2010) Basal ganglia contributions to motor control: a vigorous tutor. *Curr Opin Neurobiol* 20:704–716.
- Uno Y, Kawato M, Suzuki R (1989) Formation and control of optimal trajectory in human multijoint arm movement. minimum torque-change model. *Biol Cybern* 61:89–101.
- van Beers RJ, Haggard P, Wolpert DM (2004) The role of execution noise in movement variability. *J Neurophysiol* 91:1050–1063.
- Vetter P, Flash T, Wolpert DM (2002) Planning movements in a simple redundant task. *Curr Biol* 12:488–491.
- Wada Y, Kaneko Y, Nakano E, Osu R, Kawato M (2001) Quantitative examinations for multi joint arm trajectory planning—using a robust calculation algorithm of the minimum commanded torque change trajectory. *Neural Netw* 14:381–393.
- Wolpert DM, Ghahramani Z, Jordan MI (1995) Are arm trajectories planned in kinematic or dynamic coordinates? an adaptation study. *Exp Brain Res* 103:460–470.
- Wolpert DM, Ghahramani Z, Jordan MI (1995) An internal model for sensorimotor integration. *Science* 269:1880–1882.
- Woodworth R (1899) *The Accuracy of Voluntary Movement* Columbia University contributions to philosophy, psychology and education. Columbia University.
- Wu G, van der Helm FCT, Veeger HEJD, Makhsous M, Van Roy P, Anglin C, Nagels J, Karduna AR, McQuade K, Wang X, Werner FW, Buchholz B, ISOB (2005) Isb recommendation on definitions of joint coordinate systems of various joints for the reporting of human joint motion—part ii: shoulder, elbow, wrist and hand. *J Biomech* 38:981–992.
- Yamasaki H, Tagami Y, Fujisawa H, Hoshi F, Nagasaki H (2008) Interaction torque contributes to planar reaching at slow speed. *Biomed Eng Online* 7:27.
- Zelik KE, Kuo AD (2012) Mechanical work as an indirect measure of subjective costs influencing human movement. *PLoS One* 7: e31143.
- Zhang X, Chaffin DB (1999) The effects of speed variation on joint kinematics during multisegment reaching movements. *Human Movement Science* 18:741–757.

(Accepted 17 April 2016)
(Available online 27 April 2016)